563723

AIAA 98-0248

Hydrodynamic Instability in an Extended Landau/Levich Model of Liquid-Propellant Combustion

Stephen B. Margolis
Combustion Research Facility
Sandia National Laboratories
Livermore, California 94551-0969 USA

36th Aerospace Sciences Meeting & Exhibit
January 12–15, 1998 / Reno, NV

AIAA-98-0248

HYDRODYNAMIC INSTABILITY IN AN EXTENDED LANDAU/LEVICH MODEL OF LIQUID-PROPELLANT COMBUSTION*

STEPHEN B. MARGOLIS
Combustion Research Facility
Sandia National Laboratories
Livermore, California 94551-0969

Abstract

The classical Landau/Levich models of liquid-propellant combustion, which serve as seminal examples of hydrodynamic instability in reactive systems, have been combined and extended to account for a dynamic dependence, absent in the original formulations, of the local burning rate on the local pressure and/or temperature fields. The resulting model admits an extremely rich variety of both hydrodynamic and reactive/diffusive instabilities that can be analyzed in various limiting parameter regimes. In the present work, a formal asymptotic analysis, based on the realistic smallness of the gas-to-liquid density ratio, is developed to investigate the combined effects of gravity, surface tension and viscosity on the hydrodynamic instability of the propagating liquid/gas interface. In particular, a composite asymptotic expression, spanning three distinguished wavenumber regimes, is derived for both cellular and pulsating hydrodynamic neutral stability boundaries $A_p(k)$, where A_p is the pressure sensitivity of the burning rate and k is the disturbance wavenumber. For the case of cellular (Landau) instability, the results demonstrate explicitly the stabilizing effect of gravity on long-wave disturbances, the stabilizing effect of viscosity and surface tension on short-wave perturbations, and the instability associated with intermediate wavenumbers for critical negative values of A_p. In the limiting case of weak gravity, it is shown that cellular hydrodynamic instability in this context is a long-wave instability phenomenon, whereas at normal gravity, this instability is first manifested through O(1) wavenumber disturbances. It is also demonstrated that, in the large-wavenumber regime, surface tension and both liquid and gas viscosity all produce comparable stabilizing effects in the large-wavenumber regime, thereby providing significant modifications to previous analyses of Landau instability in which one or more of these effects were neglected. In contrast, the pulsating hydrodynamic stability boundary is found to be insensitive to gravitational and surface-tension effects, but is more sensitive to the effects of liquid viscosity, which is a significant stabilizing effect for O(1) and higher wavenumbers. Liquid-propellant combustion is predicted to be stable (i.e., steady and planar) only for a range of negative pressure sensitivities that lie between the two types of hydrodynamic stability boundaries.

1. Introduction

The burning of liquid propellants is a fundamental combustion problem that is applicable to various types of propulsion and energetic systems. The deflagration process is often rather complex, with vaporization and pyrolysis occurring at the liquid/gas interface and distributed combustion occurring either in the gas phase[1] or in a spray.[2] Nonetheless, there are realistic limiting cases in which combustion may be approximated by an overall reaction at the liquid/gas interface. In one such limit, the gas flame occurs under near-breakaway conditions, exerting little thermal or hydrodynamic influence on the burning propellant. In another such limit, distributed combustion occurs in an intrusive regime, the reaction zone lying closer to the liquid/gas interface than the length scale of any disturbance of interest. Finally, the liquid propellant may simply undergo exothermic decomposition at the surface without any significant distributed combustion, such as appears to occur in some types of hydroxylammonium nitrate (HAN)-based liquid propellants at low pressures.[3] Such limiting models have recently been formulated,[4,5] thereby significantly generalizing earlier classical models[6,7] that were originally introduced to study the hydrodynamic stability of a reactive liquid/gas interface. In all of these investigations, gravity appears explicitly and plays a significant role, along with surface tension, viscosity, and, in the more recent models, certain reaction-rate parameters associated with the pressure and temperature sensitivities of the reaction itself. In particular, these parameters determine the stability of the deflagration with respect to not only classical hydrodynamic disturbances, but also with respect to reactive/diffusive influences as well. Indeed, the inverse Froude number, representing the ratio of buoyant to inertial forces, appears explicitly in all of these models, and consequently, in the dispersion relation that determines the neutral stability boundaries beyond which steady, planar burning is unstable to nonsteady, and/or nonplanar (cellular) modes of burning.[8,9] These instabilities thus lead to a number of interesting phenomena, such as the sloshing type of waves that have been observed in mixtures of HAN and triethanolammonium nitrate (TEAN) with water.[3] Although the Froude number was treated as an O(1) or larger quantity in these studies, the limit of small inverse Froude number corresponding to the microgravity regime is increasingly of interest and can be treated explicitly, leading to various limiting forms of the models, the neutral stability boundaries, and, ultimately, the evolution equations that govern the nonlinear dynamics of the propagating reaction front.

In the present work,[15,16] we formally investigate both the normal- and reduced-gravity parameter regimes in the context of a theory that exploits the realistic smallness of the gas-to-liquid density ratio ρ. The resulting analysis and results thus facilitate a comparison of some of the features of hydrodynamic instability of liquid-propellant combustion at reduced gravity with the same phenomenon at normal gravity. In addition, the small-ρ limit allows a tractable synthesis of the separate models described in previous analyses to simultaneously account for the effects of viscosity (both liquid and gas), surface tension and pressure sensitivity of the burning rate on this phenomenon. In contrast, the original analysis of Landau[6] neglected viscosity, while that of Levich[7] retained liquid viscosity, but neglected surface tension and gas viscosity. Neither of these classical studies accounted for any variation of the local burning rate due to pressure perturbations, which has recently been introduced into this type of analysis.[4,5] The latter study, in particular, presented a highly tractable analysis of the inviscid case, thus effectively generalizing Landau's model to account for a pressure-dependent burning rate. By developing a perturbation analysis in the limit of small ρ, we show how all the phenomena just described may be simultaneously included, for both the normal and reduced gravity cases. In addition, the pressure coupling in the model predicts not only the cellular type of hydrodynamic instability attributed to Landau, but also a pulsating instability associated with sufficiently negative burning-rate pressure sensitivities. Both forms of hydrodynamic instability are analyzed here, leading to explicit asymptotic representations of the neutral stability boundaries.

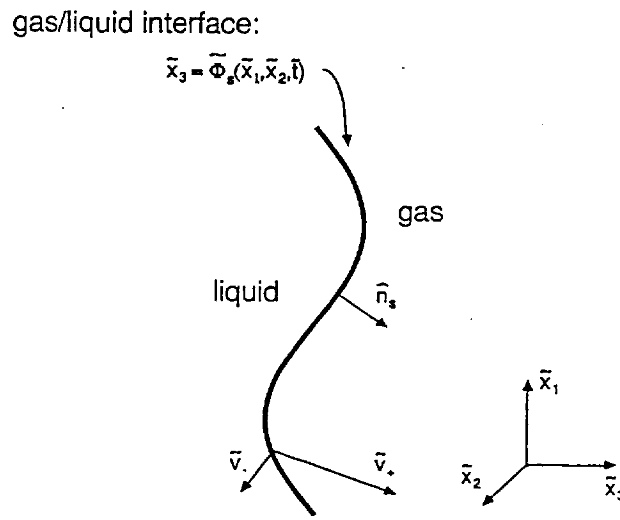

Figure 1

Model geometry. The liquid/gas interface $\tilde{x}_3 = \tilde{\Phi}_s(\tilde{x}_1, \tilde{x}_2, \tilde{t})$ *separates the unburned liquid propellant from the gaseous products.*

2. Mathematical Model

The starting point for the present work is our recent model[4,5] that generalizes classical models[6,7] of a reactive liquid/gas interface by replacing the simple assumption of a fixed normal propagation speed with a reaction/pyrolysis rate that is a function of the local pressure and temperature. This introduces important new sensitivity parameters that couple the local burning rate with the pressure and temperature fields. Thus, it is assumed, as in the classical models, that there is no distributed reaction in either the liquid or gas phases, but that there exists either a pyrolysis reaction or an exothermic decomposition at the liquid/gas interface that depends on local conditions there. In its most general form, the model includes full heat and momentum transport, allowing for viscous effects in both the liquid and gas phases, as well as effects due to gravity and surface tension. For additional simplicity, however, it is assumed that within the liquid and gas phases separately, the density, heat capacity, kinematic viscosity and thermal diffusivity are constants, with appropriate jumps in these quantities across the phase boundary.

The nondimensional location of this interface as a function of space and time is denoted by $x_3 = \Phi_s(x_1, x_2, t)$, where the adopted coordinate system is fixed with respect to the stationary liquid at $x_3 = -\infty$ (Figure 1). Then, in the moving coordinate system $x = x_1$, $y = x_2$, $z = x_3 - \Phi_s(x_1, x_2, t)$, in terms of which the liquid/gas interface always lies at $z = 0$, the complete formulation of the problem is given as follows. Conservation of mass, energy and momentum within each phase imply

$$\nabla \cdot \mathbf{v} = 0\,, \quad z \neq 0\,, \tag{1}$$

$$\frac{\partial \Theta}{\partial t} - \frac{\partial \Phi_s}{\partial t}\frac{\partial \Theta}{\partial z} + \mathbf{v}\cdot\nabla\Theta = \left\{ \begin{matrix} 1 \\ \lambda \end{matrix} \right\} \nabla^2 \Theta\,, \quad z \lessgtr 0\,, \tag{2}$$

$$\begin{aligned} \frac{\partial \mathbf{v}}{\partial t} - \frac{\partial \Phi_s}{\partial t}\frac{\partial \mathbf{v}}{\partial z} + (\mathbf{v}\cdot\nabla)\mathbf{v} &= (0,0,-Fr^{-1}) \\ - \left\{ \begin{matrix} 1 \\ \rho^{-1} \end{matrix} \right\} \nabla p &+ \left\{ \begin{matrix} Pr_l \\ \lambda Pr_g \end{matrix} \right\} \nabla^2 \mathbf{v}\,, \quad z \lessgtr 0\,, \end{aligned} \tag{3}$$

where $\mathbf{v}$, Θ and p denote velocity, temperature and pressure, respectively, Pr_l and Pr_g denote the liquid and gas-phase Prandtl numbers, ρ, λ and c (used below) are the gas-to-liquid density, thermal diffusivity and heat-capacity ratios, and Fr is the Froude number. Here, the nondimensional variables have been defined in terms of their dimensional counterparts (denoted by tildes) as

$$\begin{aligned} \mathbf{v} = \frac{\tilde{\mathbf{v}}}{\tilde{U}}\,, \quad p = \frac{\tilde{p}}{\tilde{\rho}_l \tilde{U}^2}\,, \quad \Theta = \frac{\tilde{T} - \tilde{T}_u}{\tilde{T}_a - \tilde{T}_u}\,, \\ \Phi_s = \frac{\tilde{\Phi}_s \tilde{U}}{\tilde{\lambda}_l}\,, \quad t = \frac{\tilde{t}\tilde{U}^2}{\tilde{\lambda}_l}\,, \quad x_i = \frac{\tilde{x}_i \tilde{U}}{\tilde{\lambda}_l}\,, \end{aligned} \tag{4}$$

where $\tilde{U}$ is the reference propagation speed of the interface for the case of steady, planar deflagration. The nondimensional parameters, some of which first appear below in the conditions at the gas/liquid interface (at $z = 0$), have been defined as

$$\begin{aligned} \rho = \frac{\tilde{\rho}_g}{\tilde{\rho}_l}\,, \quad \sigma_u = \frac{\tilde{T}_u}{\tilde{T}_a}\,, \quad Fr = \frac{\tilde{U}^3}{\tilde{g}\tilde{\lambda}_l}\,, \quad \gamma = \frac{\tilde{\gamma}}{\tilde{\rho}_l \tilde{\lambda}_l \tilde{U}}\,, \\ c = \frac{\tilde{c}_g}{\tilde{c}_l}\,, \quad \lambda = \frac{\tilde{\lambda}_g}{\tilde{\lambda}_l}\,, \quad Pr_l = \frac{\tilde{\nu}_l}{\tilde{\lambda}_l}\,, \quad Pr_g = \frac{\tilde{\nu}_g}{\tilde{\lambda}_g}\,, \end{aligned} \tag{5}$$

where $\tilde{T}_u$ is the unburned (liquid) temperature at $z = -\infty$ and $\tilde{T}_a$ is the adiabatic burned (gas) temperature at $z = +\infty$, $\tilde{\gamma}$ is the coefficient of surface tension for the liquid surface, and $\tilde{\nu}_l$ and $\tilde{\nu}_g$ are the liquid and gas-phase kinematic viscosities. We note that the Froude number Fr represents the ratio of inertial to buoyant (gravitational) forces, and, for future reference, that $\rho\lambda Pr_g = \mu Pr_l$, where $\mu = \tilde{\mu}_g/\tilde{\mu}_l$ is the gas-to-liquid viscosity ratio. In addition, we introduce the nondimensional mass burning rate

$$A(p|_{z=0^+}, \Theta|_{z=0}) = \tilde{A}(\tilde{p}|_{\tilde{x}_3=\tilde{\Phi}_s^+}, \tilde{T}|_{\tilde{x}_3=\tilde{\Phi}_s})/\tilde{\rho}_l\tilde{U}\,, \tag{6}$$

which is assumed to depend on the local pressure and temperature fields in the vicinity of the liquid/gas interface. Clearly, $A = 1$ for the case of steady, planar burning, but perturbations in pressure and/or temperature result in corresponding perturbations in the local mass burning rate.

Equations (1) - (3) are subject to the boundary conditions

$$\begin{aligned} &\mathbf{v} = \mathbf{0}\,, \ \Theta = 0 \ \text{at} \ z = -\infty\,, \\ &\Theta = 1 \ \text{at} \ z = +\infty\,, \quad \Theta|_{z=0^-} = \Theta|_{z=0^+} \end{aligned} \tag{7}$$

and appropriate jump and continuity conditions at the liquid/gas interface. The latter consist of continuity of the transverse velocity components (no-slip),

$$\hat{\mathbf{n}}_s \times \mathbf{v}_- = \hat{\mathbf{n}}_s \times \mathbf{v}_+\,, \tag{8}$$

where $\mathbf{v}_\pm = \mathbf{v}|_{z=0^\pm}$, conservation of (normal) mass flux,

$$\hat{\mathbf{n}}_s\cdot(\mathbf{v}_- - \rho\mathbf{v}_+) = (1-\rho)S(\Phi_s)\frac{\partial \Phi_s}{\partial t}\,, \tag{9}$$

the mass burning rate (pyrolysis) law,

$$\hat{\mathbf{n}}_s\cdot\mathbf{v}_- - S(\Phi_s)\frac{\partial \Phi_s}{\partial t} = A(p|_{z=0^+}, \Theta|_{z=0})\,, \tag{10}$$

conservation of flux of the normal and transverse components of momentum,

$$\begin{aligned} p|_{z=0^-} - p|_{z=0^+} &= \hat{\mathbf{n}}_s\cdot(\mathbf{v}_- - \rho\mathbf{v}_+)S(\Phi_s)\frac{\partial \Phi_s}{\partial t} \\ &+ \hat{\mathbf{n}}_s\cdot[\rho\mathbf{v}_+(\hat{\mathbf{n}}_s\cdot\mathbf{v}_+) - \mathbf{v}_-(\hat{\mathbf{n}}_s\cdot\mathbf{v}_-) \\ &\qquad - \rho\lambda Pr_g \mathbf{e}_+\cdot\hat{\mathbf{n}}_s + Pr_l\mathbf{e}_-\cdot\hat{\mathbf{n}}_s] \\ &- \gamma S^3(\Phi_s)\left\{\frac{\partial^2\Phi_s}{\partial x^2}\left[1 + \left(\frac{\partial \Phi_s}{\partial y}\right)^2\right]\right. \\ &\left. + \frac{\partial^2\Phi_s}{\partial y^2}\left[1 + \left(\frac{\partial \Phi_s}{\partial x}\right)^2\right] - 2\frac{\partial \Phi_s}{\partial x}\frac{\partial \Phi_s}{\partial y}\frac{\partial^2\Phi_s}{\partial x\partial y}\right\}\,, \end{aligned} \tag{11}$$

$$\begin{aligned} \hat{\mathbf{n}}_s\times\Big[\rho\mathbf{v}_+(\hat{\mathbf{n}}_s\cdot\mathbf{v}_+) &- \mathbf{v}_-(\hat{\mathbf{n}}_s\cdot\mathbf{v}_-) \\ + (\mathbf{v}_- - \rho\mathbf{v}_+)S(\Phi_s)\frac{\partial \Phi_s}{\partial t}\Big] &= \\ \hat{\mathbf{n}}_s\times(\rho\lambda Pr_g\mathbf{e}_+\cdot\hat{\mathbf{n}}_s &- Pr_l\mathbf{e}_-\cdot\hat{\mathbf{n}}_s)\,, \end{aligned} \tag{12}$$

and conservation of heat flux

$$\hat{\mathbf{n}}_s \cdot (c\rho\lambda\nabla\Theta|_{z=0^+} - \nabla\Theta|_{z=0^-}) = \hat{\mathbf{n}}_s \cdot \left[(c\rho\mathbf{v}_+ - \mathbf{v}_-)\Theta|_{z=0} + \hat{c}(\sigma_u\rho\mathbf{v}_+ - \mathbf{v}_-)\right] + \left[(1 - c\rho)\Theta|_{z=0} + \hat{c}(1 - \sigma_u\rho)\right] S(\Phi_s)\frac{\partial\Phi_s}{\partial t}, \tag{13}$$

where $\hat{c} = c/(1 - \sigma_u)$, $\mathbf{e}$ is the rate-of-strain tensor ($\mathbf{e}_\pm = \mathbf{e}|_{z=0^\pm}$), γ is the surface-tension coefficient, σ_u is the unburned-to-burned temperature ratio, and $S(\Phi_s)$ and the unit normal $\hat{\mathbf{n}}_s$ are defined as

$$S(\Phi_s) = \left[1 + (\partial\Phi_s/\partial x)^2 + (\partial\Phi_s/\partial y)^2\right]^{-1/2}, \quad \hat{\mathbf{n}}_s = (-\partial\Phi_s/\partial x, -\partial\Phi_s/\partial y, 1)S(\Phi_s). \tag{14}$$

Here, the factor multiplying γ in Eq. (11) is the curvature $-\nabla \cdot \hat{\mathbf{n}}$ of the liquid/gas interface in the moving coordinate system, and the corresponding expressions for the gradient operator ∇ and the Laplacian ∇^2 in this system are given by

$$\nabla = \left(\frac{\partial}{\partial x} - \frac{\partial\Phi_s}{\partial x}\frac{\partial}{\partial z}, \frac{\partial}{\partial y} - \frac{\partial\Phi_s}{\partial y}\frac{\partial}{\partial z}, \frac{\partial}{\partial z}\right) \tag{15}$$

and

$$\nabla^2 = \frac{\partial^2}{\partial x^2} + \frac{\partial^2}{\partial y^2} + \left[1 + \left(\frac{\partial\Phi_s}{\partial x}\right)^2 + \left(\frac{\partial\Phi_s}{\partial y}\right)^2\right]\frac{\partial^2}{\partial z^2} - 2\frac{\partial\Phi_s}{\partial x}\frac{\partial^2}{\partial x\partial z} - 2\frac{\partial\Phi_s}{\partial y}\frac{\partial^2}{\partial y\partial z} - \left(\frac{\partial^2\Phi_s}{\partial x^2} + \frac{\partial^2\Phi_s}{\partial y^2}\right)\frac{\partial}{\partial z}. \tag{16}$$

However, the vector $\mathbf{v}$ still denotes the velocity with respect to the (x_1, x_2, x_3) coordinate system. We remark that the mass burning rate A may be typically decomposed as

$$A(p|_{z=0^+}, \Theta|_{z=0}) = \hat{A}(p|_{z=0^+}, \Theta|_{z=0}) \exp\left[\frac{N(1 - \sigma_u)(\Theta|_{z=0} - 1)}{\sigma_u + (1 - \sigma_u)\Theta|_{z=0}}\right], \tag{17}$$

where $\hat{A}$ is a rate coefficient and $N = \tilde{E}/\tilde{R}^\circ\tilde{T}_a$ is the nondimensional activation energy ($\tilde{E}$). However, this more explicit representation will not be needed in the stability analysis that follows. Instead, results may be expressed in terms of the pressure and temperature sensitivities, defined as

$$A_p = \partial A/\partial p\big|_{\Theta=1,p=0}, \quad A_\Theta = \partial A/\partial\Theta\big|_{\Theta=1,p=0} = N(1 - \sigma_u) + \hat{A}_\Theta, \tag{18}$$

respectively. Finally, we note the influence of viscosity on the jump in pressure across the liquid/gas interface through the appearance of the Prandtl numbers Pr_l and Pr_g in Eq. (11). We also remark that the momentum equation (3) suggests, as noted by a reviewer, a singularity in the pressure distribution at the interface itself due to the discontinuity in velocity there. However, this singularity does not affect the *jump* in p across $z = 0$ that follows from conservation of the normal component of momentum flux, Eq. (11), which is all that is required to close the present model.

A nontrivial basic solution to the above problem, corresponding to the special case of a steady, planar deflagration, is given by

$$\Phi_s^0 = -t, \quad \Theta^0(z) = \begin{cases} e^z, & z < 0 \\ 1, & z > 0, \end{cases}$$
$$\mathbf{v}^0 = (0, 0, v^0), \quad v^0 = \begin{cases} 0, & z < 0 \\ \rho^{-1} - 1, & z > 0, \end{cases} \tag{19}$$
$$p^0(z) = \begin{cases} -Fr^{-1}z + \rho^{-1} - 1, & z < 0 \\ -\rho Fr^{-1}z, & z > 0. \end{cases}$$

The linear stability analysis of this solution now proceeds in a standard fashion. However, owing to the significant number of parameters, a complete analysis of the resulting dispersion relation is quite complex. Realistic limits that may be exploited to facilitate a perturbation analysis of the dispersion relation include $\rho \ll 1$, $\mu \ll 1$, and in the microgravity regime, $Fr^{-1} \ll 1$. In contrast, the earlier classical studies considered special limiting cases and/or assumptions. Thus, in the study due to Landau,[6] viscosity was neglected and the effects of gravity (assumed to act normal to the undisturbed planar interface in the direction of the unburned liquid) and surface tension were shown to be stabilizing, leading to a criterion for the absolute stability for steady, planar deflagration of the form (in our nondimensional notation) $4\gamma Fr^{-1}\rho^2/(1-\rho) > 1$. In the study due to Levich,[7] surface tension was neglected, but the effects due to the viscosity of the liquid were included, leading to the absolute stability criterion $Fr^{-1}Pr_l(3\rho)^{3/2} > 1$. Thus, these two studies, both of which assumed a constant normal burning rate ($A = 1$), demonstrated that sufficiently large values of either viscosity or surface tension, when coupled with the effects due to gravity, may render steady, planar deflagration stable to hydrodynamic disturbances. In the present work, these results will be synthesized and extended to the more realistic case of a nonconstant burning rate (*i.e.*, $A_p \neq 0$) in both normal and reduced gravity regimes.

3. The Hydrodynamic Linear Stability Problem

With respect to the basic solution (19), the various perturbation quantities $\phi_s(x,y,t)$, $\mathbf{u}(x,y,z,t)$, $\zeta(x,y,z,t)$ and $\theta(x,y,z,t)$ are defined as

$$\Phi_s = \Phi_s^0(t) + \phi_s\,, \quad \mathbf{v} = \mathbf{v}^0(z) + \mathbf{u}\,,$$
$$p = p^0(z) + \zeta\,, \quad \Theta = \Theta^0(z) + \theta + \phi_s \frac{d\Theta^0}{dz}\,. \tag{20}$$

Substituting Eqs. (20) into the nonlinear model (1) - (16) and linearizing about the basic solution (19), we obtain a problem for the perturbation quantities as

$$\frac{\partial u_1}{\partial x} + \frac{\partial u_2}{\partial y} + \frac{\partial u_3}{\partial z} = 0\,, \quad z \neq 0\,, \tag{21}$$

$$\begin{Bmatrix} 1 \\ \rho \end{Bmatrix} \frac{\partial \mathbf{u}}{\partial t} + \frac{\partial \mathbf{u}}{\partial z} = -\left(\frac{\partial \zeta}{\partial x} + \begin{Bmatrix} 1 \\ \rho \end{Bmatrix} Fr^{-1}\frac{\partial \phi_s}{\partial x}, \frac{\partial \zeta}{\partial y} + \begin{Bmatrix} 1 \\ \rho \end{Bmatrix} Fr^{-1}\frac{\partial \phi_s}{\partial y}, \frac{\partial \zeta}{\partial z}\right) + \begin{Bmatrix} Pr_l \\ \rho\lambda Pr_g \end{Bmatrix}\left(\frac{\partial^2 \mathbf{u}}{\partial x^2} + \frac{\partial^2 \mathbf{u}}{\partial y^2} + \frac{\partial^2 \mathbf{u}}{\partial z^2}\right), \quad z \lessgtr 0\,, \tag{22}$$

$$\begin{Bmatrix} 1 \\ \rho \end{Bmatrix} \frac{\partial \theta}{\partial t} + \frac{\partial \theta}{\partial z} = \begin{Bmatrix} -u_3\, e^z \\ 0 \end{Bmatrix} + \begin{Bmatrix} 1 \\ \rho\lambda \end{Bmatrix}\left(\frac{\partial^2 \theta}{\partial x^2} + \frac{\partial^2 \theta}{\partial y^2} + \frac{\partial^2 \theta}{\partial z^2}\right), \quad z \lessgtr 0\,, \tag{23}$$

$$\mathbf{u} = \mathbf{0}\,,\ \theta = 0 \ \text{at}\ z = -\infty\,, \qquad \theta = 0 \ \text{at}\ z = +\infty\,, \quad \theta|_{z=0^+} - \theta|_{z=0^-} = \phi_s\,, \tag{24}$$

$$u_1\big|_{z=0^-} - u_1\big|_{z=0^+} = (\rho^{-1} - 1)\frac{\partial \phi_s}{\partial x}\,, \tag{25}$$

$$u_2\big|_{z=0^-} - u_2\big|_{z=0^+} = (\rho^{-1} - 1)\frac{\partial \phi_s}{\partial y}\,, \tag{26}$$

$$u_3\big|_{z=0^-} - \rho u_3\big|_{z=0^+} = (1 - \rho)\frac{\partial \phi_s}{\partial t}\,, \tag{27}$$

$$u_3\big|_{z=0^-} - \frac{\partial \phi_s}{\partial t} = A_p \zeta|_{z=0^+} + A_\Theta \theta|_{z=0^+}\,, \tag{28}$$

$$\zeta|_{z=0^-} - \zeta|_{z=0^+} = (2-\rho)u_3\big|_{z=0^+} - u_3\big|_{z=0^-} + 2Pr_l \frac{\partial u_3}{\partial z}\bigg|_{z=0^-} - 2\rho\lambda Pr_g \frac{\partial u_3}{\partial z}\bigg|_{z=0^+} - (1-\rho)\frac{\partial \phi_s}{\partial t} - \gamma\left(\frac{\partial^2 \phi_s}{\partial x^2} + \frac{\partial^2 \phi_s}{\partial y^2}\right), \tag{29}$$

$$\rho\lambda Pr_g \left(\frac{\partial u_1}{\partial z}\bigg|_{z=0^+} + \frac{\partial u_3}{\partial x}\bigg|_{z=0^+}\right) - Pr_l \left(\frac{\partial u_1}{\partial z}\bigg|_{z=0^-} + \frac{\partial u_3}{\partial x}\bigg|_{z=0^-}\right) = (\rho^{-1} - 1)\frac{\partial \phi_s}{\partial x} + u_1\big|_{z=0^+} - u_1\big|_{z=0^-}\,, \tag{30}$$

$$\rho\lambda Pr_g \left(\frac{\partial u_2}{\partial z}\bigg|_{z=0^+} + \frac{\partial u_3}{\partial y}\bigg|_{z=0^+}\right) - Pr_l \left(\frac{\partial u_2}{\partial z}\bigg|_{z=0^-} + \frac{\partial u_3}{\partial y}\bigg|_{z=0^-}\right) = (\rho^{-1} - 1)\frac{\partial \phi_s}{\partial y} + u_2\big|_{z=0^+} - u_2\big|_{z=0^-}\,, \tag{31}$$

$$c\rho\lambda \frac{\partial \theta}{\partial z}\bigg|_{z=0^+} - \frac{\partial \theta}{\partial z}\bigg|_{z=0^-} - c\theta|_{z=0^+} + \theta|_{z=0^-} = \hat{c}\rho u_3\big|_{z=0^+} - (1+\hat{c})u_3\big|_{z=0^-} + [1 + \hat{c}(1-\rho)]\frac{\partial \phi_s}{\partial t}\,, \tag{32}$$

where $\hat{c} \equiv c(1-\sigma_u)^{-1}$.

In the present work, we shall focus, using our extended model described above, primarily on hydrodynamic (Landau) instability. Thus, in the linear stability analysis, we retain only the pressure sensitivity A_p in the perturbation of the pyrolysis law (10), neglecting the temperature sensitivity A_Θ. The latter assumption thus filters out reactive/diffusive instabilities associated with the thermal coupling of the temperature field,[4,5] but greatly facilitates the analysis of instability due to hydrodynamic effects alone. We note that the mass burning rate of many propellants has been shown empirically to correlate well with pressure.

Nontrivial harmonic solutions for ϕ_s, $\mathbf{u}$ and ζ, proportional to $e^{i\omega t + ik_1 x + ik_2 y}$, that satisfy Eqs. (21) - (22) and the boundary/boundedness conditions at $z = \pm\infty$ are given by

$$\phi_s = e^{i\omega t + ik_1 x + ik_2 y}\,, \tag{33}$$

$$\zeta = e^{i\omega t + ik_1 x + ik_2 y} \begin{cases} b_1 e^{kz} - Fr^{-1} \\ b_2 e^{-kz} - \rho Fr^{-1}\,, \end{cases} \tag{34}$$

$$u_1 = e^{i\omega t + ik_1 x + ik_2 y} \begin{cases} b_3 e^{qz} - ik_1(i\omega + k)^{-1} b_1 e^{kz} \\ b_4 e^{rz} - ik_1(i\omega\rho - k)^{-1} b_2 e^{-kz}, \end{cases} \tag{35}$$

$$u_2 = e^{i\omega t + ik_1 x + ik_2 y} \begin{cases} b_5 e^{qz} - ik_2(i\omega + k)^{-1} b_1 e^{kz} \\ b_6 e^{rz} - ik_2(i\omega\rho - k)^{-1} b_2 e^{-kz}, \end{cases} \tag{36}$$

$$u_3 = e^{i\omega t + ik_1 x + ik_2 y} \begin{cases} b_7 e^{qz} - k(i\omega + k)^{-1} b_1 e^{kz} \\ b_8 e^{rz} + k(i\omega\rho - k)^{-1} b_2 e^{-kz}, \end{cases} \tag{37}$$

for $z \lessgtr 0$, where we have normalized the above solution by setting the coefficient of the harmonic dependence of ϕ_s to unity. Here, the signs of k_1 and k_2 may be either positive or negative and we have employed the definition $k = \sqrt{k_1^2 + k_2^2}$, and q and r are defined as

$$2Pr_l\, q = 1 + \sqrt{1 + 4Pr_l(i\omega + Pr_l\, k^2)}\,, \tag{38}$$

$$2\mu Pr_l\, r = 1 - \sqrt{1 + 4\mu Pr_l(i\omega\rho + \mu Pr_l\, k^2)}\,, \quad (39)$$

where we have used the fact, noted below Eq. (5), that $\rho\lambda Pr_g = \mu Pr_l$.

Substituting this solution into the interface conditions (25) - (31) and using Eq. (21) for $z \lessgtr 0$ yields nine conditions for the eight coefficients b_1 - b_8 and the complex frequency (dispersion relation) $i\omega(k)$. In particular, these conditions are given by

$$ik_1 b_3 + ik_2 b_5 + q b_7 = 0\,, \quad (40)$$

$$ik_1 b_4 + ik_2 b_6 + r b_8 = 0\,, \quad (41)$$

$$b_3 - \frac{ik_1}{i\omega + k} b_1 - b_4 + \frac{ik_1}{i\omega\rho - k} b_2 = \Big(\frac{1}{\rho} - 1\Big) ik_1\,, \quad (42)$$

$$b_5 - \frac{ik_2}{i\omega + k} b_1 - b_6 + \frac{ik_2}{i\omega\rho - k} b_2 = \Big(\frac{1}{\rho} - 1\Big) ik_2\,, \quad (43)$$

$$b_7 - \frac{k}{i\omega + k} b_1 - \rho b_8 - \frac{\rho k}{i\omega\rho - k} b_2 = (1-\rho) i\omega\,, \quad (44)$$

$$b_7 - \frac{k}{i\omega + k} b_1 - A_p\, b_2 = i\omega - \rho Fr^{-1} A_p\,, \quad (45)$$

$$\begin{aligned}&\Big[1 + \frac{k}{i\omega + k}(2kPr_l - 1)\Big] b_1 \\ &- \Big[1 + \frac{k}{i\omega\rho - k}(2k\mu Pr_l + 2 - \rho)\Big] b_2 \\ &+ (1 - 2Pr_l\, q) b_7 - (2 - \rho - 2\mu Pr_l\, r) b_8 = \\ &\qquad (1-\rho)(Fr^{-1} - i\omega) + \gamma k^2\,,\end{aligned} \quad (46)$$

$$\begin{aligned}&(\mu Pr_l\, r - 1) b_4 + (2k\mu Pr_l + 1)\frac{ik_1}{i\omega\rho - k} b_2 \\ &+ ik_1 \mu Pr_l\, b_8 + (1 - Pr_l\, q) b_3 - ik_1 Pr_l\, b_7 \\ &+ (2Pr_l\, k - 1)\frac{ik_1}{i\omega + k} b_1 = \Big(\frac{1}{\rho} - 1\Big) ik_1\,,\end{aligned} \quad (47)$$

$$\begin{aligned}&(\mu Pr_l\, r - 1) b_6 + (2k\mu Pr_l + 1)\frac{ik_2}{i\omega\rho - k} b_2 \\ &+ ik_2 \mu Pr_l\, b_8 + (1 - Pr_l\, q) b_5 - ik_2 Pr_l\, b_7 \\ &+ (2Pr_l\, k - 1)\frac{ik_2}{i\omega + k} b_1 = \Big(\frac{1}{\rho} - 1\Big) ik_2\,.\end{aligned} \quad (48)$$

While the above problem is linear in the coefficients b_1 - b_8, the relationship for $i\omega$ is highly nonlinear. Accordingly, we ultimately will exploit the fact that the gas-to-liquid density and viscosity ratios ρ and μ are typically small, as is Fr^{-1} in the case of reduced gravity, and seek an asymptotic representation of the dispersion relation in this parameter regime. As we shall see, this distinguished limit simplifies the problem by inducing three distinct wavenumber regimes that can be analyzed individually. Consequently, it is possible to develop separate perturbation expansions for the neutral stability boundaries in each of these wavenumber regimes, which can then be combined using asymptotic matching principles to produce a uniformly valid composite expression for each boundary.

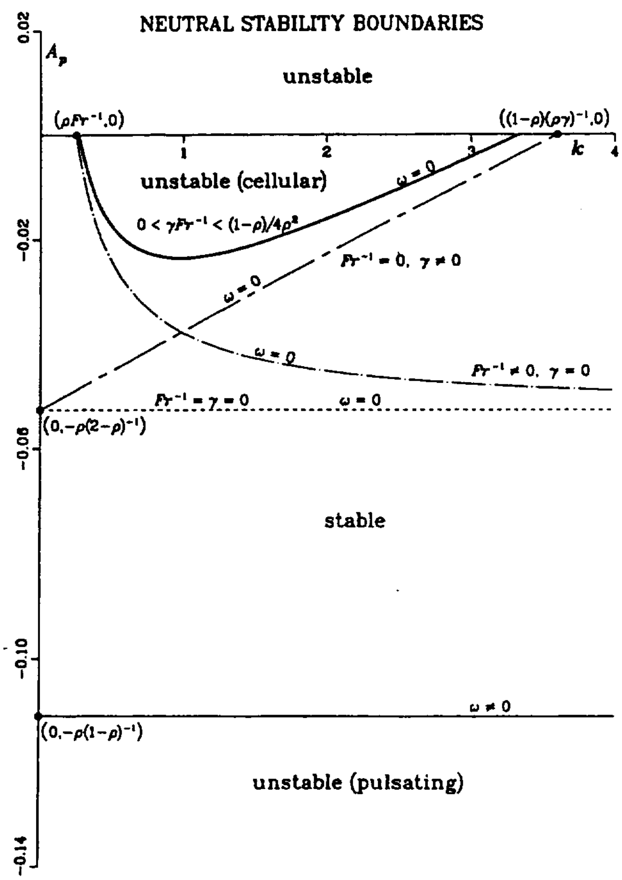

Figure 2

Hydrodynamic neutral stability boundaries in the limit of zero viscosity.

4. Hydrodynamic Instability: Zero-Viscosity Limit

Although both liquid and gas-phase viscous effects will be shown to be comparable in general to those due to surface tension, the inviscid limit provides a particularly tractable limiting case and motivates the scalings to be used in the asymptotic analysis of the fully viscous problem. Thus, in the limit of zero viscosities ($Pr_l = Pr_g = 0$), our extended model differs from the classical one due to Landau[6] only in the local pressure sensitivity of the normal burning rate. In that limit, the dispersion relation with respect to infinitesimal hydrodynamic disturbances proportional to $e^{i\omega t \pm i\mathbf{k}\cdot\mathbf{x}}$, where $\mathbf{k}$ and $\mathbf{x}$ are the transverse wavenumber and coordinate vectors, respectively, is determined as[5]

$$\begin{aligned} &A_p\rho^2(1-\rho)(i\omega)^3 - \rho^2 k\left[1+\rho+A_p(1-\rho)\right](i\omega)^2 \\ &+\rho k\left\{A_p\left[\rho(1+\rho)Fr^{-1}+\rho k^2\gamma-(1-\rho)k\right]\right. \\ &\qquad\qquad\left.-2\rho k\right\}(i\omega) \\ &+A_p k^2\left[(1-\rho)(2-\rho)k+\rho^2(3-\rho)Fr^{-1}+\rho^2k^2\gamma\right] \\ &\quad+\rho k^2\left[(1-\rho)k-\rho(1-\rho)Fr^{-1}-\rho k^2\gamma\right]=0 . \end{aligned} \tag{49}$$

The corresponding neutral stability boundaries are easily determined explicitly and are exhibited in Figure 2. Steady, planar burning is always unstable for positive values of A_p, but in the region $A_p \le 0$, there exist both cellular ($\omega = 0$) and pulsating ($\omega \neq 0$) stability boundaries $A_p(k;\rho,\gamma,Fr^{-1})$ given by

$$A_p = \frac{\rho\left[\rho(1-\rho)Fr^{-1}+\rho\gamma k^2-(1-\rho)k\right]}{\rho^2(3-\rho)Fr^{-1}+\rho^2\gamma k^2+(1-\rho)(2-\rho)k} \le 0, \quad \omega = 0 , \tag{50}$$

and

$$A_p = -\frac{\rho}{1-\rho}, \quad \omega^2 = k\left[\frac{1+\rho}{1-\rho}Fr^{-1}+\frac{k^2}{1-\rho}\gamma+\frac{k}{\rho}\right], \tag{51}$$

respectively, where $k = |\mathbf{k}|$. Steady, planar combustion is therefore stable in the region $A_p < 0$ that lies between these two curves, where the pulsating stability boundary is a straight line in the (A_p, k) plane and the cellular stability boundary is a curve which lies above the former in the region $A_p \ge -\rho/(2-\rho)$. The shape of the latter boundary depends on whether or not the parameters Fr^{-1} and/or γ are zero. In the limit that the product γFr^{-1} approaches the value $(1-\rho)/4\rho^2$ from below, the cellular stability boundary recedes from the region $A_p < 0$. For $\gamma Fr^{-1} > (1-\rho)/4\rho^2$, the stable region is the strip $-\rho/(1-\rho) < A_p < 0$. Thus, when $A_p = 0$, the classical Landau result for cellular instability is recovered. However, even a small positive value of A_p renders steady, planar burning intrinsically unstable for all disturbance wavenumbers, regardless of the stabilizing effects of gravity and surface tension, since there always exists a positive real root of Eq. (49) for $A_p > 0$ (for small ρ, this root is given by $i\omega \sim k/A_p$). This result may be anticipated from quasi-steady physical considerations. That is, a burning velocity that increases with increasing pressure is a hydrodynamically unstable situation, since an increase in the burning velocity results in an increase in the pressure jump across the liquid/gas interface, and vice-versa. However, a sufficiently large negative value of A_p results in a pulsating hydrodynamic instability, the existence of which was a new prediction for liquid-propellant combustion. Zero and negative values of A_p over certain pressure ranges are characteristic of the so-called "plateau" and "mesa" types of solid propellants,[10] as well as for the HAN-based liquid propellants mentioned above.[3]

Of particular interest in the present work is the cellular hydrodynamic, or Landau, instability of liquid-propellant combustion in the limit of small gravitational effects (in microgravity, for example). In this limit, the shape of the upper hydrodynamic stability boundary in Figure 2, corresponding to the classical type of instability that was first described by Landau,[6] clearly approximates the $Fr^{-1} = 0$ curve except for small wavenumbers, where, unless the inverse Froude number is identically zero, the neutral stability boundary must turn and intersect the horizontal axis. Consequently, the neutral stability boundary has a minimum for some small value of the transverse wavenumber k of the disturbance, implying loss of stability of the basic solution to long wavelength perturbations as the pressure sensitivity A_p defined above decreases in magnitude. This, in turn, suggests a small wavenumber nonlinear stability analysis in the unstable regime, which generally leads to simplified nonlinear evolution equations of the Kuramoto-Sivashinsky type for the finite amplitude perturbations.[11,12]

To establish the nature of hydrodynamic instability in the microgravity regime in a formal sense, as well as to introduce a formalism whereby the analysis of the fully viscous case may be simplified, we may realistically consider the parameter regime $\rho \ll 1$, $Fr^{-1} \ll 1$, with $Fr^{-1} \sim \rho$. For example, typical values are $\rho \sim 10^{-3} - 10^{-4}$, liquid thermal diffusivity $\tilde{\lambda}_l \sim 0.1\ \mathrm{m^2/sec}$, and the steady, planar burning rate $\tilde{U} \sim 1 - 10$ cm/sec depending on pressure.[3] Hence, from the definition $Fr^{-1} \equiv \tilde{g}\tilde{\lambda}_l/\tilde{U}^3$, we conclude that $Fr^{-1} \sim \rho$ implies that the dimensional gravitational acceleration $\tilde{g} \lesssim 10^{-5}\mathrm{m/sec^2}$, which, roughly speaking, marks the onset of the microgravity regime. Thus, introducing the bookkeeping parameter $\epsilon \ll 1$, we define scaled parameters g^*, ρ^* and A_p^* according to

$$\rho = \rho^*\epsilon, \quad A_p = A_p^*\epsilon, \quad Fr^{-1} = \begin{cases} g \\ g^*\epsilon \end{cases}, \tag{52}$$

with γ remaining an O(1) parameter. Here, the lower scaling on Fr^{-1} corresponds to the reduced gravity limit, whereas the upper definition indicates the normal gravity case. In both regimes, it is readily seen from Eq. (50) that there are three distinct wavenumber scales that must be considered in order to properly account for the relative magnitude of the various terms in the numerator and denominator in the expression for A_p. In particular, in addition to the O(1), or outer, scale k, there is an inner scale k_i and a far outer scale k_f that are respectively defined as

$$k_i = \begin{cases} k/\epsilon, & Fr^{-1} \sim O(1) \\ k/\epsilon^2, & Fr^{-1} \sim O(\epsilon) \end{cases}, \qquad k_f = k\epsilon. \quad (53)$$

In the thin inner and thick far outer regions, we thus readily obtain

$$A_p^* \sim A_p^{*(i)} \sim \begin{cases} \rho^*(\rho^* g - k_i)/2k_i \\ \rho^*(\rho^* g^* - k_i)/2k_i \end{cases}, \quad (54)$$

and

$$A_p^* \sim A_p^{*(f)} \sim \frac{1}{2}\rho^*(\rho^*\gamma k_f - 1), \quad (55)$$

respectively. Each of these two expansions may be matched to the O(1) outer expansion, which is given by

$$A_p^* \sim A_p^{*(o)} \sim -\frac{1}{2}\rho^*, \quad (56)$$

and thus a uniformly valid composite expansion, denoted by $A_p^{*(c)}(k)$, may be constructed as

$$A_p^{*(c)} \sim A_p^{*(i)} + A_p^{*(o)} + A_p^{*(f)} - \lim_{k_i \to \infty} A_p^{*(i)} - \lim_{k_f \to 0} A_p^{*(f)} \sim -\frac{1}{2}\rho^* + \frac{1}{2}\epsilon\rho^{*2}\gamma k + \begin{cases} \epsilon\rho^{*2} g/2k \\ \epsilon^2\rho^{*2} g^*/2k \end{cases}, \quad (57a)$$

where the definitions of k_i and k_f have been used to express the final result in terms of k (Figure 3). In terms of the original unscaled parameters, Eq. (57a) beomes

$$A_p \sim -\frac{\rho}{2} + \frac{\rho^2\gamma k}{2} + \frac{\rho^2 Fr^{-1}}{2k}, \quad (57b)$$

which eliminates the small scaling parameter ϵ from the composite expansion. Noting the simplicity of the asymptotic result (57) relative to the exact expression given in Eq. (50), it is easily seen that the hydrodynamic stability boundary in the regime considered here lies in the region $A_p^* \leq 0$, intersecting the $A_p^* = 0$ axis at

$$k = k_1 \sim \frac{1}{\rho^*\gamma\epsilon} \gg 1 \quad (58)$$

and at

$$k = k_2 \sim \begin{cases} \rho^* g\epsilon \\ \rho^* g^* \epsilon^2 \end{cases} \ll 1, \quad (59)$$

with a single local minimum at

$$k = \hat{k} \sim \begin{cases} \sqrt{g/\gamma} \\ \sqrt{\epsilon g^*/\gamma} \end{cases} \sim \sqrt{Fr^{-1}/\gamma} \sim \begin{cases} O(1) \\ O(\sqrt{\epsilon}) \end{cases}, \quad (60)$$

corresponding to the critical value

$$A_p^* = \hat{A}_p^* \sim -\frac{1}{2}\rho^* + \begin{cases} \epsilon\rho^{*2}\sqrt{g\gamma} \\ \epsilon\rho^{*2}\sqrt{\epsilon g^*\gamma} \end{cases}. \quad (61a)$$

Thus, in terms of the unscaled parameters, instability first occurs for disturbances at the critical value

$$A_p = \hat{A}_p \sim -\frac{1}{2}\rho + \rho^2\sqrt{\gamma Fr^{-1}}. \quad (61b)$$

The essential difference, as illustrated by Figure 3, between the normal and reduced gravity limits in

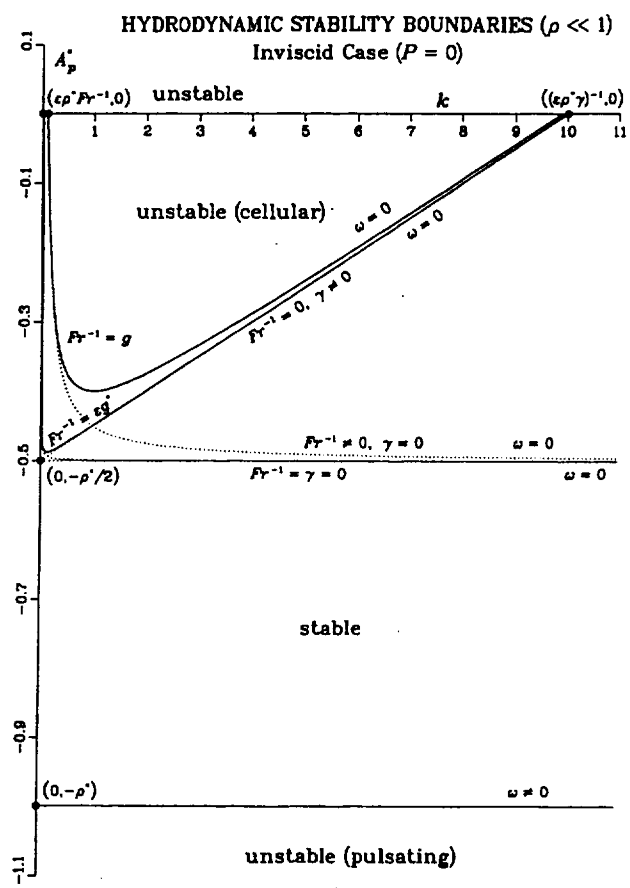

Figure 3

Asymptotic representation of the cellular hydrodynamic neutral stability boundary in the limit of zero viscosity. The upper (lower) solid curves correspond to the two cases described by Eqs. (57) for normal and reduced-gravity, respectively (curves are drawn for the case $\epsilon = 0.04$, $\rho^* = 1.0$, $g = 2.5$, $g^* = 1.0$*).*

the realistic parameter regime considered here is that in the latter instance, gravity is only capable of stabilizing disturbances whose wavenumbers are very small, $O(\epsilon^2)$, whereas in the former case, gravity is sufficiently strong to stabilize disturbances whose wavenumbers are $O(\epsilon)$. As a consequence, hydrodynamic instability becomes a long-wave instability phenomenon in the reduced gravity regime considered here, since the most unstable wavenumbers are $O(\sqrt{\epsilon})$, rather than $O(1)$, in that case. We note that the role of surface tension, on the other hand, serves to stabilize only short-wave disturbances, which are, to this order of approximation, unaffected by the magnitude of the gravitational acceleration.

5. Hydrodynamic Instability: Fully Viscous Case

Guided by these results for the inviscid case, the linear stability analysis may be extended to include the effects of viscosity as follows. Retaining the scalings (52), we have noted that $\rho\lambda Pr_g = \mu Pr_l$, where $\mu = \mu_g/\mu_l$ is the gas-to-liquid viscosity ratio. Thus, it is reasonable to treat $Pr_l \equiv P$ as an $O(1)$ parameter, and to consider the limit

$$\mu = \mu^* \epsilon \ll 1 . \tag{62}$$

Introducing the scalings (52) and (62) directly into Eqs. (40) – (48), approximate solutions for the coefficients may be sought in the form of appropriate expansions in powers of ϵ. As suggested by the inviscid analysis, it is necessary to construct separate expansions for the inner, outer and far outer wavenumber regimes defined above. Since we are interested in obtaining the hydrodynamic cellular stability boundary, we may set $i\omega$ equal to zero directly and seek solutions for b_1 – b_8 and A_p^*, where the latter expressed as a function of k will describe the stability boundary. Forms for the various expansions are suggested in part by the corresponding solutions for these coefficients in the inviscid limit (for which exact solutions are analytically tractable[5]).

In the $O(1)$ wavenumber regime, the expansions for q and r are, from Eqs. (38) and (39),

$$r \sim r_1 \epsilon + \cdots , \quad r_1 = \mu^* P k^2 , \tag{63}$$

$$q \sim q_0 + \cdots , \quad q_0 = \frac{1 + \sqrt{1 + 4P^2k^2}}{2P} , \tag{64}$$

and appropriate expansions for the coefficients b_1 – b_8 and A_p are given by

$$b_i \sim b_i^{(-1)} \epsilon^{-1} + b_i^{(0)} + b_i^{(1)} \epsilon + \cdots , \quad i = 2,\ 8 , \tag{65}$$

$$b_i \sim b_i^{(0)} + b_i^{(1)} \epsilon + \cdots , \quad i = 1,\ 3,\ 4,\ 5,\ 6,\ 7 , \tag{66}$$

$$A_p = A_p^{*(o)} \epsilon \sim \epsilon (A_0^{*(o)} + A_1^{*(o)} \epsilon + \cdots) . \tag{67}$$

Substituting these expansions and the scalings (52) and (62) into Eqs. (40) – (48), and collecting coefficients of like powers of ϵ, we obtain a sequence of algebraic problems for the coefficients in Eqs. (65) – (67). In particular, from either of Eqs. (42) and (43), we obtain

$$b_2^{(-1)} = -k/\rho^* , \tag{68}$$

and the leading-order versions of Eqs. (44) – (46) are given by

$$b_7^{(0)} - b_1^{(0)} - \rho^* b_8^{(-1)} + \rho^* b_2^{(-1)} = 0 , \tag{69}$$

$$b_7^{(0)} - b_1^{(0)} - A_0^{*(o)} b_2^{(-1)} = 0 , \tag{70}$$

$$b_2^{(-1)} - 2 b_8^{(-1)} = 0 . \tag{71}$$

Subtracting Eqs. (69) and (70), and using Eqs. (68) and (71) for $b_2^{(-1)}$ and $b_8^{(-1)}$, we obtain the result

$$A_0^{*(o)} = -\frac{1}{2}\rho^* . \tag{72}$$

Equations (67) and (72) are equivalent to the inviscid result (56) in the outer wavenumber regime, and thus, to the leading order of approximation, viscosity does not affect the neutral stability boundary for $O(1)$ disturbance wavenumbers.

A corresponding result is obtained in the inner wavenumber regime defined by the first of Eqs. (53). In particular, the expansions for q and r are now given by

$$r \sim \mu^* P k_i^2 \begin{cases} \epsilon^3 + \cdots \\ \epsilon^5 + \cdots \end{cases} , \quad q \sim \frac{1}{2P} + P k_i^2 \begin{cases} \epsilon^2 + \cdots \\ \epsilon^4 + \cdots \end{cases} , \tag{73}$$

and the expansions for the coefficients b_1 – b_8 and A_p may be sought in the form

$$b_i \sim \begin{cases} b_i^{(0)} + b_i^{(1)} \epsilon + \cdots \\ b_i^{(1)} \epsilon + b_i^{(2)} \epsilon^2 + \cdots , \end{cases} \quad i = 2,\ 8 , \tag{74}$$

$$b_i \sim \begin{cases} b_i^{(1)} \epsilon + b_i^{(2)} \epsilon^2 + \cdots \\ b_i^{(1)} \epsilon^2 + b_i^{(3)} \epsilon^3 + \cdots \end{cases} , \quad i = 1,\ 3,\ 4,\ 5,\ 6, \tag{75}$$

$$A_p = A_p^{*(i)} \epsilon \sim \epsilon (A_0^{*(i)} + A_1^{*(i)} \epsilon + \cdots) . \tag{76}$$

Substituting these expansions and the scalings (52) and (62) into Eqs. (40) – (48) as before, we again obtained a much-simplified set of algebraic equations at each order. In the reduced-gravity regime, for example, we obtain from Eq. (40) and either of Eqs. (42) or (43) that

$$b_7^{(2)} = 0 , \quad b_2^{(1)} = -\frac{k_i}{\rho^*} , \tag{77}$$

while Eqs. (44) – (46) give

$$b_7^{(2)} - b_1^{(2)} - \rho^* b_8^{(1)} + \rho^* b_2^{(1)} = 0\,, \qquad (78)$$

$$b_7^{(2)} - b_1^{(2)} - A_0^{*(i)} b_2^{(1)} = 0\,, \qquad (79)$$

$$b_2^{(1)} - 2b_8^{(1)} = g^*\,. \qquad (80)$$

An identical set is obtained in the normal-gravity regime in terms of the leading-order coefficients in the expansions (74) and (75) for that case, with the exception that g^* is replaced by its unscaled counterpart g in Eq. (80). Subtracting Eqs. (78) and (79) and using the results (77) and (80), we thus obtain

$$A_0^{*(i)} \sim \begin{cases} \rho^*(\rho^* g - k_i)/2k_i \\ \rho^*(\rho^* g^* - k_i)/2k_i \end{cases}, \qquad (81)$$

which is again equivalent to the inviscid result (54). Thus, to leading order, neither the inner nor the outer wavenumber regimes are influenced by viscous effects. Indeed, to a first approximation, viscosity is only significant for large-wavenumber disturbances, as we shall now demonstrate.

In the far outer wavenumber regime defined by the second of Eqs. (53), the expansions for q and r are given by

$$r \sim r_{(-1)}\,\epsilon^{-1} + \cdots, \quad r_{(-1)} = \frac{1 - (1 + 4\mu^{*2} P^2 k_f^2)^{1/2}}{2\mu^* P}, \qquad (82)$$

$$q \sim q_{(-1)}\,\epsilon^{-1} + \cdots, \quad q_{(-1)} = k_f\,, \qquad (83)$$

and appropriate expansions for the coefficients b_1 – b_8 and A_p are given by

$$b_i \sim b_i^{(-1)}\epsilon^{-1} + b_i^{(0)} + \cdots, \quad i = 1, 3, 5, 7, \qquad (84)$$

$$b_i \sim b_i^{(-2)}\epsilon^{-2} + b_i^{(-1)}\epsilon^{-1} + \cdots, \quad i = 2, 4, 6, 8, \qquad (85)$$

$$A_p = A_p^{*(f)}\epsilon \sim \epsilon(A_0^{*(f)} + A_1^{*(f)}\epsilon + \cdots)\,. \qquad (86)$$

Substituting these latest expansions into Eqs. (40) – (48), we obtain the leading-order system

$$ik_{1f}\, b_3^{(-1)} + ik_{2f}\, b_5^{(-1)} + q_{(-1)}\, b_7^{(-1)} = 0\,, \qquad (87)$$

$$ik_{1f}\, b_4^{(-2)} + ik_{2f}\, b_6^{(-2)} + r_{(-1)}\, b_8^{(-2)} = 0\,, \qquad (88)$$

$$-b_4^{(-2)} - \frac{ik_{1f}}{k_f} b_2^{(-2)} = \frac{ik_{1f}}{\rho^*}\,, \qquad (89)$$

$$-b_6^{(-2)} - \frac{ik_{2f}}{k_f} b_2^{(-2)} = \frac{ik_{2f}}{\rho^*}\,, \qquad (90)$$

$$b_7^{(-1)} - b_1^{(-1)} - \rho^* b_8^{(-2)} + \rho^* b_2^{(-2)} = 0\,, \qquad (91)$$

$$b_7^{(-1)} - b_1^{(-1)} - A_0^{*(f)} b_2^{(-2)} = 0\,, \qquad (92)$$

$$2k_f P b_1^{(-1)} + (1 + 2k_f \mu^* P) b_2^{(-2)} - 2P\, q_{(-1)} b_7^{(-1)} - 2(1 - \mu^* P\, r_{(-1)}) b_8^{(-2)} = \gamma k_f^2\,, \qquad (93)$$

$$(\mu^* P\, r_{(-1)} - 1) b_4^{(-2)} - (2k_f \mu^* P + 1)\frac{ik_{1f}}{k_f} b_2^{(-2)} + ik_{1f}\mu^* P b_8^{(-2)} - P\, q_{(-1)} b_3^{(-1)} + 2ik_{1f} P b_1^{(-1)} - ik_{1f} P b_7^{(-1)} = \frac{ik_{1f}}{\rho^*}\,, \qquad (94)$$

$$(\mu^* P\, r_{(-1)} - 1) b_6^{(-2)} - (2k_f \mu^* P + 1)\frac{ik_{2f}}{k_f} b_2^{(-2)} + ik_{2f}\mu^* P b_8^{(-2)} - P\, q_{(-1)} b_5^{(-1)} + 2ik_{2f} P b_1^{(-1)} - ik_{2f} P b_7^{(-1)} = \frac{ik_{2f}}{\rho^*}\,, \qquad (95)$$

where, analogous to the scaling for k in the far outer regime, $k_{1f} = k_1\epsilon$ and $k_{2f} = k_2\epsilon$. Equations (87) – (95) may be solved for the leading-order coefficients in Eqs. (84) – (86) such that, after some algebra (Appendix A), we obtain the result

$$A_0^{*(f)} = -\frac{\rho^*}{r_{(-1)}}\left[(k_f + r_{(-1)}) + \frac{(r_{(-1)} + k_f)(1 + 2\rho^* P k_f) + k_f}{\rho^*\gamma\, r_{(-1)} - 2\rho^* P k_f - 2(1 - \mu^* P\, r_{(-1)})}\right], \qquad (96)$$

which may be rewritten as

$$A_0^{*(f)} \sim -\rho^* + \frac{2\rho^*\mu^* P\,[1 + k_f(\rho^*\gamma + 2\mu^* P + 2\rho^* P)]}{4\mu^* P(1 + \rho^* P k_f) - [1 - R(k_f)](\rho^*\gamma + 2\mu^* P)}, \quad R(k_f) = \left[1 + 4\mu^{*2} P^2 k_f^2\right]^{1/2}. \qquad (97)$$

It is readily observed that both the liquid *and* the gas-phase viscosities (through the parameters P and $\mu^* P$, respectively) enter into this expression, reflecting an equal influence of viscous and surface-tension effects on the neutral stability boundary in the large-wavenumber regime. The equal importance of gas-phase viscosity relative to that of the liquid phase stems from the fact that gas-phase disturbances are, according to Eqs. (84) and (85), larger in magnitude than those in the liquid phase, such that a weak damping of a larger magnitude disturbance is of equal importance to an O(1) damping of a smaller magnitude disturbance. In the limit $P \to 0$, the inviscid expression (55) is recovered. It is easily shown that

$$\lim_{k_f \to 0} A_0^{*(f)} = -\frac{1}{2}\rho^*\,, \qquad (98)$$

so that the far outer solution can be matched to the outer solution (72). As k_f increases, $A_0^{*(f)}$ increases, intersecting the $A_0^{*(f)} = 0$ axis at the value $k_f = \hat{k}_f$ given by

$$\hat{k}_f = \frac{1}{\rho^*\gamma}\left(1 - \frac{\mu^* P}{\rho^*\gamma + 2\mu^* P}\right), \qquad (99)$$

which agrees with the inviscid result for $\rho^* \ll 1$ in the limit $\mu^* P \to 0$. As this boundary crosses the horizontal axis, it must eventually reach a maximum and decrease to $A_0^{*(f)} = 0$, since $\lim_{k_f\to\infty} A_0^{*(f)} = 0$. However, as indicated earlier in the discussion of the inviscid case, there is another root $i\omega \sim O(\epsilon^{-2})$ that takes on positive values for $A_p^* > 0$ (Appendix B). Consequently, only that portion of the hydrodynamic stability boundary that lies below the horizontal axis ($A_0^* = 0$) is relevant to our discussion.

A uniformly valid composite expansion spanning all three wavenumber regimes described above may be constructed as in Eqs. (57), giving the result

$$A_p^{*(c)} \sim -\rho^* + \frac{\rho^{*2}}{2k}\begin{cases}\epsilon g \\ \epsilon^2 g^*\end{cases} + \frac{2\rho^*\mu^* P\left[1 + \epsilon k(\rho^*\gamma + 2\mu^* P + 2\rho^* P)\right]}{4\mu^* P(1 + \epsilon k\rho^* P) - (\rho^*\gamma + 2\mu^* P)\left[1 - R(\epsilon k)\right]}, \qquad (100a)$$

or, reverting to the unscaled parameters A_p, ρ, μ and Fr^{-1},

$$A_p^{*(c)} \sim -\rho + \frac{\rho^2}{2k}Fr^{-1} + \frac{2\rho\mu P\left[1 + k(\rho\gamma + 2\mu P + 2\rho P)\right]}{4\mu P(1 + k\rho P) - (\rho\gamma + 2\mu P)\left[1 - R(k)\right]}, \qquad (100b)$$

which again eliminates the small bookkeeping parameter ϵ from the problem. Both the normal and reduced gravity boundaries $A_p^{*(c)}(k)$ are graphically exhibited in Figure 4 for various zero and representative nonzero values of μ^*, P, Fr^{-1} and γ. It is readily seen that the essential qualitative difference between the normal and reduced-gravity curves is the location of the critical wavenumber for instability. Specifically, the minimum in the neutral stability boundaries occurs for O(1) values of k under normal gravity, and at $k \sim O(\epsilon^{1/2})$ in the reduced-gravity limit considered here, as in the inviscid case described above. Indeed, it may be shown that Eqs. (100) collapse to Eqs. (57) in the limit of zero viscosity ($P = 0$), but we again note that viscous effects in *both* the liquid (P) and gas ($\mu^* P$) are comparable to surface-tension effects (γ) in damping large-wavenumber disturbances. In fact, it is clear from Figure 4 that increasing the values of any of the parameters P, $\mu^* P$ or γ serves to shrink the size of the unstable domain through damping of short-wave perturbations. The non-negligible effects of

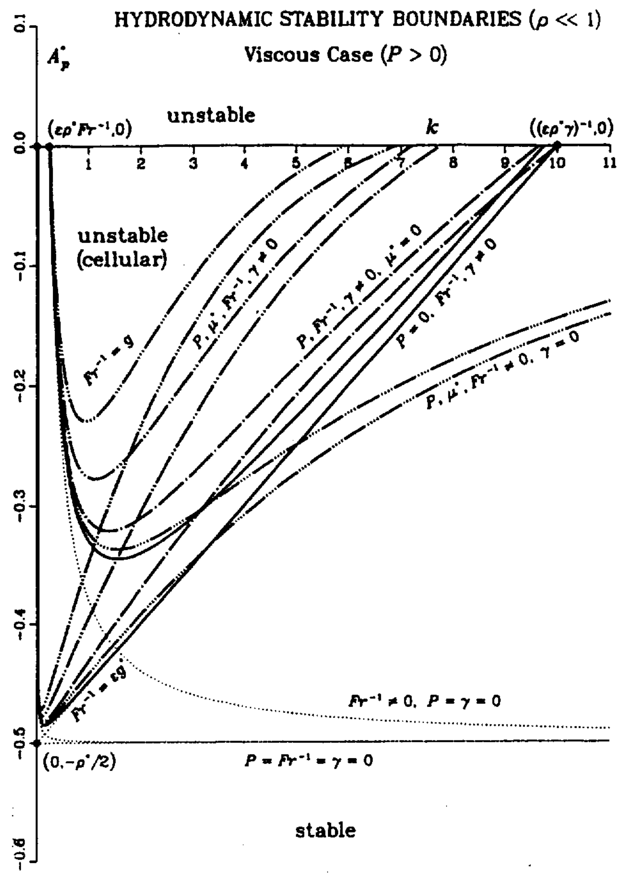

Figure 4

Asymptotic representation of the cellular hydrodynamic neutral stability boundary for the viscous case. The upper and lower sets of curves correspond to the normal and reduced-gravity regimes, respectively, in the asymptotic limit considered in this work (curves drawn for the case $\epsilon = .04$, $\rho^* = 1.0$, $g = 6.0$, $g^* = 2.0$). The solid curves correspond to the inviscid limit ($P = 0$) with nonzero surface tension ($\gamma = 2.5$). The dash-dot curves correspond to nonzero surface tension ($\gamma = 2.5$) and liquid viscosity ($P = 1.0$), but zero gas-phase viscosity ($\mu^* P = 0$). The dash-dot-dot curves differ from the dash-dot curves by the addition of gas-phase viscosity ($\mu^* P = 1.0$), and are similar to the dash-dot-dot-dot curves, where the latter correspond to larger viscosities ($P = \mu^* P = 2.0$). The dash-dot-dot-dot-dot curves correspond to a viscous case ($P = \mu^* P = 1.0$), but with zero surface tension ($\gamma = 0$), so that, from Eq. (99), the curves do not intercept the $A_p^* = 0$ axis.

gas-phase viscosity represents an important correction to Levich's original treatment[7] in which these effects were simply assumed to be small. The result (100a,b) thus synthesizes and significantly extends the classical Landau/Levich results,[6,7] not only in allowing for a dynamic dependence of the burning rate on local conditions in the vicinity of the liquid/gas interface, but also in its formal treatment of those processes (surface tension, liquid and gas-phase viscosity) that affect damping of large-wavenumber disturbances.

6. Asymptotic Analysis of the Pulsating Stability Boundary

As indicated previously, the existence of a nonstationary pressure dependence on the burning rate (i.e., $A_p \neq 0$) leads to the prediction of a pulsating hydrodynamic stability boundary that is absent when such a pressure coupling is neglected, as in the original Landau/Levich theories. In the inviscid case, this boundary (39) is a straight line that lies below the cellular boundary discussed above, but this is modified under the influence of viscosity, as we shall demonstrate.

For the scalings (52) and (62) adopted in the preceding sections [in particular, for $P \sim O(1)$, $\mu \sim O(\epsilon)$], it turns out that, unlike the cellular stability boundary where viscous effects only have a leading-order effect in the far outer wavenumber regime, the effects of viscosity have a leading-order effect on the pulsating boundary for O(1) wavenumbers as well. Thus, in the outer wavenumber region, we seek a solution for the dispersion relation in the form

$$i\omega \sim \epsilon^{-1/2}(i\omega_0 + i\omega_1\epsilon^{1/4} + i\omega_2\epsilon^{1/2} + \cdots), \quad (101)$$

where the leading-order term is suggested by the explicit results for the inviscid case,[4,5] and the expansion in powers of $\epsilon^{1/4}$ is suggested by the expansions for r and q, which, from Eqs. (38) and (39), have the form

$$\begin{aligned} r &\sim r_{(1/2)}\epsilon^{1/2} + r_{(3/4)}\epsilon^{3/4} + r_1\epsilon + \cdots, \\ &\quad r_{(1/2)} = -i\omega_0\rho^*, \quad r_{(3/4)} = -i\omega_1\rho^*, \\ &\quad r_1 = -i\omega_2\rho^* - (\mu^* Pk)^2, \end{aligned} \quad (102)$$

$$\begin{aligned} q &\sim q_{(-1/4)}\epsilon^{-1/4} + q_0\epsilon^0 + \cdots, \\ &\quad q_{(-1/4)} = \sqrt{i\omega_0/P}, \quad q_0 = \frac{1 + i\omega_1/\sqrt{i\omega_0/P}}{2P}. \end{aligned} \quad (103)$$

Corresponding expansions for the coefficients b_i in Eqs. (40) – (48) are determined as

$$b_i = b_i^{(-1)}\epsilon^{-1} + b_i^{(-3/4)}\epsilon^{-3/4} + b_i^{(-1/2)}\epsilon^{-1/2} + \cdots, \quad i = 1, 2, 8, \quad (104)$$

$$b_i = b_i^{(-1/2)}\epsilon^{-1/2} + b_i^{(-1/4)}\epsilon^{-1/4} + \cdots, \quad i = 3, 4, 5, 6, \quad (105)$$

$$b_i = b_i^{(-1/4)}\epsilon^{-1/4} + b_i^{(0)}\epsilon^0 + \cdots, \quad i = 7, \quad (106)$$

where the leading terms in the expansions for b_1, b_2, b_4, b_6 and b_8 are consistent with the inviscid results[5] and the remaining coefficients appear only for nonzero values of P and are conservatively postulated to have the indicated expansions. Substituting these expansions into Eqs. (40) – (48) and equating coefficients of like powers of ϵ, we obtain the leading-order equations/results

$$ik_1\, b_3^{(-1/2)} + ik_2\, b_5^{(-1/2)} + q_{(-1/4)}\, b_7^{(-1/4)} = 0, \quad (107)$$

$$ik_1\, b_4^{(-1/2)} + ik_2\, b_6^{(-1/2)} + r_{(1/2)}\, b_8^{-1} = 0, \quad (108)$$

$$b_2^{(-1)} = -\frac{k}{\rho^*}, \quad (109)$$

$$b_1^{(-1)} = \frac{(i\omega_0)^2}{k}, \quad (110)$$

$$b_8^{(-1)} = -\left(1 + \frac{A_p^*}{\rho^*}\right)\frac{k}{\rho^*}, \quad (111)$$

$$b_1^{(-1)} + b_2^{(-1)} - 2b_8^{(-1)} = 0, \quad (112)$$

where Eq. (111) was obtained from the leading-order difference of Eqs. (44) and (45), and the remainder of the leading-order versions of Eqs. (40) – (48) give redundant results. Substituting Eqs. (109) – (111) into Eq. (112), we obtain

$$(i\omega_0)^2 = \frac{k^2}{\rho^*}\left(1 + 2\frac{A_p^*}{\rho^*}\right), \quad (113)$$

and thus $(i\omega_0)^2 \gtrless 0$ for $A_p^* \gtrless -\rho^*/2$, which essentially recovers the leading-order cellular stability boundary (56) for O(1) wavenumbers, but gives no information on the pulsating boundary since $i\omega_0$ is purely imaginary for $A_p^* < -\rho^*/2$. Hence, stability in the latter region is determined by higher-order coefficients in the expansion (101) for $i\omega$.

Continuing with the analysis of the expanded forms of Eqs. (40) – (48), we obtain the second-order equations/results

$$ik_1\, b_3^{(-1/4)} + ik_2\, b_5^{(-1/4)} + q_{(-1/4)}\, b_7^{(0)} + q_0\, b_7^{(-1/4)} = 0, \quad (114)$$

$$ik_1\, b_4^{(-1/4)} + ik_2\, b_6^{(-1/4)} + r_{(1/2)}\, b_8^{(-3/4)} + r_{(3/4)}\, b_8^{(-1)} = 0\,, \tag{115}$$

$$b_2^{(-3/4)} = 0\,, \tag{116}$$

$$k\, b_2^{(-1/2)} - q_{(-1/4)} b_7^{(-1/4)} = i\omega_0 k \left(1 - \frac{A_p^*}{\rho^*}\right)\,, \tag{117}$$

$$b_7^{(-1/4)} - \frac{k}{i\omega_0} b_1^{(-3/4)} = i\omega_1\,, \tag{118}$$

$$b_8^{(-3/4)} = 0\,, \tag{119}$$

$$b_1^{(-3/4)} = 2b_8^{(-3/4)} = 0\,, \tag{120}$$

$$b_3^{(-1/2)} = b_5^{(-1/2)} = 0\,, \tag{121}$$

where Eq. (117) was obtained from the sum of Eq. (42) multiplied by ik_1 and Eq. (43) multiplied by ik_2 and the use of Eq. (107), Eq. (119) was obtained from the difference of Eqs. (44) and (45), and Eqs. (121) follow from Eqs. (47) and (48) in conjunction with Eq. (116). From these results and Eq. (107), we thus conclude that

$$b_7^{(-1/4)} = i\omega_1 = 0\,, \quad b_2^{(-1/2)} = i\omega_0 \left(1 - \frac{A_p^*}{\rho^*}\right)\,, \tag{122}$$

where the fact that $i\omega_1 = 0$ implies the need to calculate $i\omega_2$ to determine stability in the region $A_p^* < -\rho^*/2$. Proceeding in this fashion, we obtain from the next-order versions of Eqs. (44), (46), the difference of Eqs. (44) and (45), and the sum of Eq. (47) multiplied by ik_1 and Eq. (48) multiplied by ik_2, the relations

$$b_7^{(0)} - \frac{k}{i\omega_0} b_1^{(-1/2)} + \frac{i\omega_2 + k}{(i\omega_0)^2} k\, b_1^{(-1)} - \rho^* b_8^{(-1)} + \rho^* b_2^{(-1)} = i\omega_2\,, \tag{123}$$

$$b_1^{(-1/2)} + \frac{k}{i\omega_0}(2Pk - 1) b_1^{(-1)} + b_2^{(-1/2)} + \frac{2i\omega_0 \rho^*}{k} b_2^{(-1)} - 2b_8^{(-1/2)} = -i\omega_0\,, \tag{124}$$

$$-\rho^* b_8^{(-1/2)} + \rho^* b_2^{(-1/2)} + \frac{i\omega_0 \rho^{*2}}{k} b_2^{(-1)} + A_p^* b_2^{(-1/2)} = -i\omega_0 \rho^*\,, \tag{125}$$

$$-i\omega_0 \rho^* b_8^{(-1)} + k\, b_2^{(-1/2)} + i\omega_0 \rho^* b_2^{(-1)} + i\omega_0 b_7^{(0)} - (2Pk - 1)\frac{k^2}{i\omega_0} b_1^{(-1)} = 0\,, \tag{126}$$

which, in combination with the expressions for $b_1^{(-1)}$, $b_2^{(-1)}$, $b_8^{(-1)}$, $b_2^{(-1/2)}$ and $i\omega_0$ given above, constitute four equations for the four unknowns $b_1^{(-1/2)}$, $b_7^{(0)}$, $b_8^{(-1/2)}$ and $i\omega_2$. Solving these simultaneous equations, we thus obtain

$$b_7^{(0)} = -2Pk^2\,,$$
$$b_1^{(-1/2)} = \left[2Pk + 1 + \frac{A_p^*}{\rho^*} - 2\left(\frac{A_p^*}{\rho^*}\right)^2\right] i\omega_0\,, \tag{127}$$
$$b_8^{(-1/2)} = \left[1 - \left(\frac{A_p^*}{\rho^*}\right)^2\right] i\omega_0\,,$$

$$i\omega_2 = k\left[\left(\frac{A_p^*}{\rho^*}\right)^2 - 2Pk - 1\right]\,. \tag{128}$$

Equation (128) is the desired result, from which we conclude that $i\omega_2 \lesssim 0$ for $(A_p^*/\rho^*)^2 \lesssim 1 + 2Pk$. Thus, in the region $A_p^* < 0$, $i\omega_2$ vanishes on the boundary

$$A_p^* \sim -\rho^* \sqrt{1 + 2Pk}\,, \tag{129}$$

which is a pulsating boundary (Fig. 5) since, from Eq. (113), $i\omega_0$ is purely imaginary along this curve.

Equation (129) is valid for O(1) wavenumbers, but since it matches to the leading-order inviscid inner pulsating boundary $A_p^* = -\rho^*$ as $k \to 0$, and becomes large in a negative sense as k becomes large, it is clear that Eq. (129) represents the pulsating boundary for arbitrary wavenumbers. That is, for $P \sim O(1)$, the effects of (liquid) viscosity on the pulsating boundary are, to a first approximation, absent for small wavenumbers, are first felt for O(1) wavenumber perturbations, and are sufficient to move this boundary to larger-magnitude values $A_p^* \sim O(\epsilon^{-1/2})$ in the far outer wavenumber regime. In contrast, the cellular boundary (100) is unaffected for O(1) and smaller wavenumbers, and is only modified an O(1) amount for $O(\epsilon^{-1})$ wavenumbers, where both gas and liquid viscosities are equally significant. Thus, the hydrodynamic pulsating boundary is more sensitive to liquid viscous effects than is the corresponding cellular stability boundary. In fact, even for smaller-magnitude viscosities such that $P \sim O(\epsilon^{1/2}$ (with $\mu \sim O(\epsilon)$ as above), it is easily demonstrated (see Appendix C) that, in the A_p regime considered here, the pulsating boundary is eliminated in the far outer wavenumber region. However, for even smaller liquid viscosities such that $P = \hat{P}\epsilon \sim O(\epsilon)$, it may be shown by a completely analogous calculation (Appendix D) to the one given above that O(1) modifications to the pulsating boundary then occur in the far outer wavenumber regime according to $A_p^* = -\rho^*\left(1 + 2\hat{P}k_f\right)^{1/2}$, which, in terms of unscaled quantities, is the same as Eq. (129).

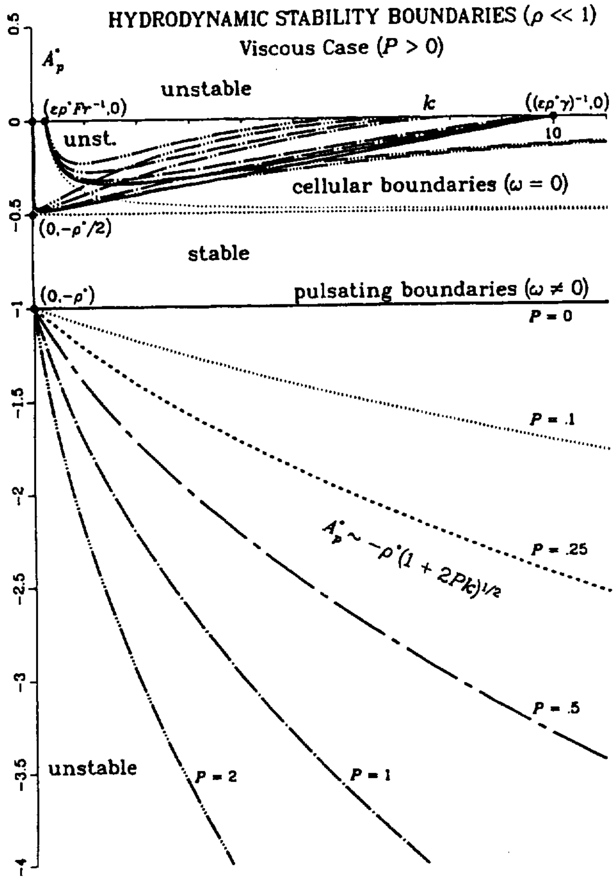

Figure 5

Asymptotic representation of the pulsating hydrodynamic neutral stability boundary for the viscous case ($P > 0$). The region between the pulsating and cellular boundaries (the latter are shown on an expanded scale in Fig. 4) is the stable region with respect to hydrodynamic instability.

Other cellular and pulsating stability boundaries are obtained for nonzero values of the temperature sensitivity parameter A_Θ, and are thus of a reactive/diffusive nature since they arise from a coupling of the burning rate to the local temperature field. These have been analyzed in the realistic limit $\rho \ll 1$ for the inviscid case,[5] and the generalization of these results to the fully viscous problem in both the normal and reduced-gravity regimes is currently under investigation. One important result obtained from the inviscid analysis is that a nonzero value of the thermal sensitivity A_Θ appears to have little effect on the hydrodynamic cellular stability boundary shown in Figures 2 – 4. This result suggests that the upper stability boundary in Figure 2, corresponding to the onset of steady cells on the propellant surface, is especially likely to be observable. Indeed, an analysis of nonlinear stability in the neighborhood of this boundary[8,9] not only confirms the existence of steady cellular structures above this boundary, but also demonstrates how the interaction of certain types of cellular modes can result in secondary and tertiary transitions to time-periodic motions[11,13,14] that may also correspond to the sloshing type of behavior observed in HAN/TEAN/water mixtures.[3]

7. Conclusion

The present work has presented a formal asymptotic analysis of hydrodynamic instability in liquid-propellant combustion for a surface model in which burning takes place at the liquid/gas interface. The model itself is based on a synthesized version of the classical models analyzed by Landau[6] and Levich,[7] but generalized to allow a coupling of the mass burning rate with the local pressure and/or temperature fields.[4,5] Focusing on the pressure-coupled version of the model, the realistic smallness of the gas-to-liquid density ratio was shown to be a convenient small parameter upon which to base an asymptotic treatment, resulting in three distinct wavenumber regimes such that different physical processes assume dominance in each. Both cellular and pulsating hydrodynamic stability boundaries are predicted, the former corresponding to Landau's original notion of hydrodynamic instability, and the latter representing a new prediction arising from the pressure dependence of the burning rate. For the cellular type of instability, it was shown that the gravitational acceleration (assumed to be normal to the undisturbed liquid/gas interface in the direction of the liquid) is responsible for stabilizing long-wave disturbances, whereas surface tension and viscosity are effective in stabilizing short-wave perturbations. As a consequence, reduced gravity results in a shift in the minimum of the neutral stability boundary towards smaller wavenumbers, such that the onset of hydrodynamic instability, predicted to occur for sufficiently small negative values of the pressure-sensitivity coefficient A_p, becomes a long-wave instability in that limit. An additional result is that gas-phase viscosity plays an equally significant role as does liquid viscosity in the large-wavenumber regime. This important effect, absent from previous treatments, stems from the fact that gas-phase disturbances are larger in magnitude than those in the liquid phase. That is, although the gas-to-liquid viscosity ratio is small, a weak damping of a larger magnitude disturbance is of equal importance to an O(1) damping of a smaller magnitude disturbance. The inclusion of both viscous and surface-tension effects in a single analysis, which are of comparable importance for short-wave perturbations thus represents an important synthesis of the classical Landau/Levich theories of hydrodynamic instability.

In the case of the pulsating hydrodynamic instability that arises from the pressure coupling that exists in the generalized model analyzed here, we find that neither gravity nor surface tension play a leading-order role, and viscous effects are the dominant stabilizing influence. Indeed, for O(1) liquid Prandtl numbers, the stabilizing effects of (liquid) viscosity on pulsating instability are significant for disturbances whose wavenumbers are O(1) or larger. In contrast, it was shown that viscous effects are only significant for large-wavenumber disturbances in the case of cellular instability, where the influence of gas and liquid viscosity are comparable despite the small ratio of these two parameters. Although the onset of pulsating hydrodynamic instability is predicted to occur only for sufficiently negative values of the pressure-sensitivity coefficient A_p, the persistence of the pulsating stability boundary (in the presence of viscous effects) for small wavenumbers suggests that it may be observable in those types of liquid propellants, such as those based on hydroxylammonium nitrate (HAN) and/or triethanolammonium nitrate (TEAN), that are characterized by negative pressure sensitivities over certain pressure ranges. However, in attempting to interpret the sloshing behavior that has been observed during combustion of certain HAN/TEAN/water mixtures,[3] we note that nonsteady burning can arise via secondary and other higher-order bifurcations in the cellular instability region,[11,13,14] as well as from a primary crossing of the pulsating boundary. Hence, further measurements are generally needed to determine the precise origin of such behavior in any given experiment.

Appendix A. Derivation of $A_0^{*(f)}(k_f)$

The steps leading to Eq. (96) for the neutral stability boundary in the outer wavenumber regime are as follows. First, from Eqs. (89) and (90), we obtain expressions for $b_4^{(-2)}$ and $b_6^{(-2)}$ in terms of $b_2^{(-2)}$. Substituting these results into Eq. (88) then determines $b_8^{(-2)}$ in terms of $b_2^{(-2)}$ as well, so that

$$\begin{aligned} b_4^{(-2)} &= -ik_{1f}\left(\frac{b_2^{(-2)}}{k_f}+\frac{1}{\rho^*}\right),\\ b_6^{(-2)} &= -ik_{2f}\left(\frac{b_2^{(-2)}}{k_f}+\frac{1}{\rho^*}\right),\\ b_8^{(-2)} &= -\frac{k_f}{r_{(-1)}}\left(b_2^{(-2)}+\frac{k_f}{\rho^*}\right). \end{aligned} \quad (A.1)$$

Using this last expression for $b_8^{(-2)}$ in the equation obtained from subtracting Eq. (92) from Eq. (91), thus determines the neutral stability boundary in terms of $b_2^{(-2)}$ as

$$A_0^{*f} = -\rho^*\left(\frac{k_f}{r_{(-1)}}+1\right)-\frac{k_f^2}{r_{(-1)}b_2^{(-2)}}. \quad (A.2)$$

Using the last of Eqs. (A.1), we now solve Eq. (91) for $b_7^{(-1)}$ in terms of $b_1^{(-1)}$ and $b_2^{(-2)}$,

$$b_7^{(-1)} = b_1^{(-1)}-\rho^* b_2^{(-2)}\left(\frac{k_f}{r_{(-1)}}+1\right)-\frac{k_f^2}{r_{(-1)}}, \quad (A.3)$$

and using this result along with the first two of Eqs. (A.1) in Eqs. (94) and (95) leads to the relations

$$\begin{aligned} &b_2^{(-2)}\left[\rho^*\left(1+\frac{k_f}{r_{(-1)}}\right)-\mu^*\left(\frac{k_f}{r_{(-1)}}+2+\frac{r_{(-1)}}{k_f}\right)\right] - \frac{k_f}{ik_{1f}}b_3^{(-1)}+b_1^{(-1)} = \\ &\qquad -\frac{k_f^2}{r_{(-1)}}+\frac{\mu^*}{\rho^*}\left(r_{(-1)}+\frac{k_f^2}{r_{(-1)}}\right), \end{aligned} \quad (A.4)$$

$$\begin{aligned} &b_2^{(-2)}\left[\rho^*\left(1+\frac{k_f}{r_{(-1)}}\right)-\mu^*\left(\frac{k_f}{r_{(-1)}}+2+\frac{r_{(-1)}}{k_f}\right)\right] - \frac{k_f}{ik_{2f}}b_5^{(-1)}+b_1^{(-1)} = \\ &\qquad -\frac{k_f^2}{r_{(-1)}}+\frac{\mu^*}{\rho^*}\left(r_{(-1)}+\frac{k_f^2}{r_{(-1)}}\right). \end{aligned} \quad (A.5)$$

Subtracting Eq. (A.5) from Eq. (A.4), we obtain

$$\frac{b_5^{(-1)}}{ik_{2f}} = \frac{b_3^{(-1)}}{ik_{1f}}, \quad (A.6)$$

which, when substituted into Eq. (87), gives

$$b_7^{(-1)} = \frac{k_f}{ik_{1f}}b_3^{-1} = \frac{k_f}{ik_{2f}}b_5^{-1}. \quad (A.6)$$

Finally, substituting Eq. (A.3) and the last of Eqs. (A.1) into Eq. (93) and using the fact, from Eq. (83), that $q_{(-1)} = k_f$, we completely determine $b_2^{(-2)}$ as

$$b_2^{(-2)} = \frac{k_f^2}{\rho^*} \cdot \frac{\rho^* \gamma r_{(-1)} - 2\rho^* P k_f - 2(1 - \mu^* P r_{(-1)})}{(r_{(-1)} + k_f)(1 + 2\rho^* P k_f) + k_f} \,. \tag{A.7}$$

The remaining coefficients may now be solved for explicitly. For example, $b_4^{(-2)}$, $b_6^{(-2)}$ and $b_8^{(-2)}$ are now determined according to Eqs. (A.1), while the use of Eq. (A.7) for $b_2^{(-2)}$ and the first of Eqs. (A.6) for $b_7^{(-1)}$ reduces Eqs. (A.3) and (A.4) to two simultaneous equations for $b_1^{(-1)}$ and $b_3^{(-1)}$. Furthermore, when Eq. (A.7) is substituted into Eq.(A.2), we obtain the desired expression (96) for $A_0^{*(f)}$.

Appendix B. Intrinsic Instability for $A_p^* > 0$

A direct analysis of the dispersion relation (49) corresponding to the inviscid case indicates that, in addition to the roots that lead to the stability boundaries (50) and (51), there is an additional root that, for $\rho \sim O(\epsilon) \ll 1$ and $k \sim O(1)$, is given by $i\omega \sim \epsilon^{-1} k / A_p^*$.[5] It may be shown that this result is valid in the inner and far outer wavenumber regimes as well, so that, at least in the inviscid case, the region $A_p^* > 0$ is intrinsically unstable. Based on the results in Section 5 for the viscous case, we may anticipate that the only possible modification to this result will occur in the far outer wavenumber regime $k = k_f/\epsilon$, which we now consider.

Thus, we seek a root of the dispersion relation implied by the system (87) – (95) that has the asymptotic behavior in the far outer wavenumber regime given by

$$i\omega \sim \epsilon^{-2}(i\omega_0 + i\omega_1 \epsilon + \cdots) \,, \tag{B.1}$$

whereas, based on the inviscid results, the roots of the dispersion relation that leads to the cellular stability boundary (97) in the far outer regime behave as $O(\epsilon^{-3/2})$. Thus, corresponding to Eq. (B.1), the expressions for $r_{(-1)}$ and $q_{(-1)}$ in the expansions (82) – (83) for r and q are now given by

$$r_{(-1)} = \frac{1}{2\mu^* P}\left[1 - \sqrt{1 + 4\mu^* P(i\omega_0 \rho^* + \mu^* P k_f^2)}\,\right] \,,$$
$$q_{(-1)} = \frac{1}{P}\sqrt{P(i\omega_0 + P k_f^2)} \,, \tag{B.2}$$

whereas the appropriate expansions for the coefficients b_i are now written as

$$b_i \sim b_i^{(-2)} \epsilon^{-2} + b_i^{(-1)} \epsilon^{-1} + \cdots \,, \quad i = 3, 5, 7 \,, \tag{B.3}$$

$$b_i \sim b_i^{(-3)} \epsilon^{-3} + b_i^{(-2)} \epsilon^{-2} + \cdots \,, \quad i = 1, 2, 4, 6, 8 \,. \tag{B.4}$$

Hence, in place of Eqs. (87) – (95), the leading-order coefficients and the root $i\omega_0$ are determined from Eqs. (40) – (48) by

$$i k_{1f} b_3^{(-2)} + i k_{2f} b_5^{(-2)} + q_{(-1)} b_7^{(-2)} = 0 \,, \tag{B.5}$$

$$i k_{1f} b_4^{(-3)} + i k_{2f} b_6^{(-3)} + r_{(-1)} b_8^{(-3)} = 0 \,, \tag{B.6}$$

$$-b_4^{(-3)} + \frac{i k_{1f}}{i\omega_0 \rho^* - k_f} b_2^{(-3)} = 0 \,, \tag{B.7}$$

$$-b_6^{(-3)} + \frac{i k_{2f}}{i\omega_0 \rho^* - k_f} b_2^{(-3)} = 0 \,, \tag{B.8}$$

$$b_7^{(-2)} - \frac{k_f}{i\omega_0} b_1^{(-3)} - \rho^* b_8^{(-3)} - \frac{\rho^* k_f}{i\omega_0 \rho^* - k_f} b_2^{(-3)} = i\omega_0 \,, \tag{B.9}$$

$$b_7^{(-2)} - \frac{k_f}{i\omega_0} b_1^{(-3)} - A_p^* b_2^{(-3)} = i\omega_0 \,, \tag{B.10}$$

$$\begin{aligned}&\left(1 + \frac{2k_f^2}{i\omega_0} P\right) b_1^{(-3)} \\ &\quad - \left[1 + \frac{2k_f}{i\omega_0 \rho^* - k_f}(k_f \mu^* P + 1)\right] b_2^{(-3)} \\ &\quad - 2P\, q_{(-1)} b_7^{(-2)} - 2(1 - \mu^* P r_{(-1)}) b_8^{(-3)} = 0 \,,\end{aligned} \tag{B.11}$$

$$\begin{aligned}&(\mu^* P r_{(-1)} - 1) b_4^{(-3)} - P\, q_{(-1)} b_3^{(-2)} \\ &\quad + (2k_f \mu^* P + 1) \frac{i k_{1f}}{i\omega_0 \rho^* - k_f} b_2^{(-3)} + i k_{1f} \mu^* P b_8^{(-3)} \\ &\quad + 2P k_f \frac{i k_{1f}}{i\omega_0} b_1^{(-3)} - i k_{1f} P b_7^{(-2)} = 0 \,,\end{aligned} \tag{B.12}$$

$$\begin{aligned}&(\mu^* P r_{(-1)} - 1) b_6^{(-3)} - P\, q_{(-1)} b_5^{(-2)} \\ &\quad + (2k_f \mu^* P + 1) \frac{i k_{2f}}{i\omega_0 \rho^* - k_f} b_2^{(-3)} + i k_{2f} \mu^* P b_8^{(-3)} \\ &\quad + 2P k_f \frac{i k_{2f}}{i\omega_0} b_1^{(-3)} - i k_{2f} P b_7^{(-2)} = 0 \,.\end{aligned} \tag{B.13}$$

The dispersion relation for $i\omega_0$ is now obtained as follows. From Eqs. (B.6) – (B.8), we have

$$b_4^{(-3)} = \frac{i k_{1f}}{i\omega_0 \rho^* - k_f} b_2^{(-3)} \,, \quad b_6^{(-3)} = \frac{i k_{2f}}{i\omega_0 \rho^* - k_f} b_2^{(-3)} \,,$$
$$b_8^{(-3)} = \frac{k_f^2}{r_{(-1)}(i\omega_0 \rho^* - k_f)} b_2^{(-3)} \,, \tag{B.14}$$

Hence, substituting the last of Eqs. (B.14) into the difference of Eqs. (B.9) and (B.10), and canceling the common factor $b_2^{(-3)}$, we arrive at the dispersion relation

$$-\frac{\rho^* k_f}{i\omega_0\rho^* - k_f}\left(\frac{k_f}{r_{(-1)}} + 1\right) + A_p^* = 0\,, \qquad (B.15)$$

or

$$(i\omega_0\rho^* - k_f)r_{(-1)}A_p^* - \rho^* k_f r_{(-1)} - \rho^* k_f^2 = 0\,, \; (B.16)$$

where we note that in going from Eq. (B.15) to Eq. (B.16), the extraneous root $i\omega_0 = k_f/\rho^*$ has been introduced into the dispersion relation. It is readily shown that for $\mu^* P \ll 1$, $r_{(-1)} \sim -i\omega_0\rho^*$. Substituting the latter into Eq. (B.16), we obtain a quadratic for $i\omega_0$ which has the roots k_f/A_p^* and the extraneous root k_f/ρ^*. Thus, for $\mu^* P \ll 1$, we recover the inviscid result $i\omega_0 \sim k_f/A_p^*$, indicating instability for $A_p^* > 0$.

For the viscous case $\mu^* P \sim \mathrm{O}(1)$, we substitute the expression for $r_{(-1)}$ given in the first of Eqs. (B.2) into Eq. (B.16), and after squaring to eliminate the square root and factoring out the extraneous factor $(i\omega_0\rho^* - k_f)$ noted above, we are left with the dispersion relation

$$\alpha^2 + [(\mu^* P k_f - 1)A_p^* - 2\rho^*]\alpha + \rho^*(A_p^* + \rho^*) - \mu^* P k_f A_p^*(A_p^* + 2\rho^*) = 0\,, \qquad (B.17)$$

where $\alpha \equiv i\omega_0\rho^* A_p^*/k_f$. Solving for α and choosing the nonextraneous root (the one that collapses to the inviscid result in the inviscid limit), we finally obtain

$$i\omega_0 = \frac{k_f}{A_p^*} + \frac{k_f}{2\rho^* A_p^*}\cdot\begin{cases} A_p^*(1 - \mu^* P k_f) - \Omega(A_p^*, k_f), & A_p^* > 0 \\ A_p^*(1 - \mu^* P k_f) + \Omega(A_p^*, k_f), & A_p^* < 0, \end{cases}$$
$$\Omega(A_p^*, k_f) = \sqrt{(A_p^*)^2(1 + \mu^* P k_f)^2 + 4\rho^*\mu^* P k_f A_p^*}\,. \qquad (B.18)$$

It is clear from Eq. (B.16) that for sufficiently small $\mu^* P$ and/or $|A_p^*|$, $i\omega_0 \gtrless 0$ for $A_p^* \gtrless 0$. We also observe that $i\omega_0 \sim k_f/A_p^*$ as $k_f \to 0$, indicating that the inviscid result is recovered as the outer wavenumber regime is approached. Although this root can turn negative for sufficiently large A_p^* (indeed, $i\omega_0 = 0$ for $2\mu^* P k_f A_p^*/\rho^* = 1 - 2\mu^* P k_f + \sqrt{1 + 4\mu^{*2} P^2 k_f^2} > 0$), this region is of little further interest since hydrodynamic instability first sets in for negative values of A_p^*.

Appendix C. Effect of Viscosity on the Hydrodynamic Pulsating Stability Boundary for $k \gg 1$

The existence of the pulsating stability boundary (51) obtained from the inviscid analysis is highly sensitive to viscous effects. Indeed, it is easily shown that, in the far outer wavenumber region where viscous effects are first felt, a weakly nonzero value of the liquid-phase Prandtl number P, while producing no leading-order effect on the inviscid cellular boundary, is sufficient to eliminate the pulsating type of hydrodynamic instability. Thus, we retain the scalings (52) and (62), but consider the weakly viscous case

$$P = P^*\sqrt{\epsilon}\,, \quad \mu P = \mu^* P^* \epsilon^{3/2} \qquad (C.1)$$

where the choice of scaling (C.1) permits the same scalings for $i\omega$ and those coefficients b_i (i = 1, 2, 4, 6, 8) that apply in the inviscid limit. Thus, based on the inviscid analysis of the dispersion relation (49), we seek corresponding roots $i\omega$ for the weakly viscous problem in the far outer wavenumber region $k = k_f/\epsilon$ in the form

$$i\omega \sim \epsilon^{-3/2}(i\omega_0 + i\omega_1\epsilon^{1/2} + \cdots)\,, \qquad (C.2)$$

where, in contrast to the expansion (B.1) in the region $A_p^* > 0$, this form of the expansion will describe both the cellular and pulsating hydrodynamic instabilities in the region $A_p^* < 0$.

In the far outer wavenumber region $k = k_f/\epsilon$, the expansions for r and q are given by

$$r \sim r_{(-1/2)}\epsilon^{-1/2} + r_0\epsilon^0 + \cdots\,;$$
$$r_{(-1/2)} = -i\omega_0\rho^* - \mu^* P^* k_f^2\,, \quad r_0 = -i\omega_1\rho^*\,, \qquad (C.3)$$

$$q \sim q_{(-1)}\epsilon^{-1} + q_{(-1/2)}\epsilon^{-1/2} + \cdots\,;$$
$$q_{(-1)} = \left(i\omega_0/P^* + k_f^2\right)^{1/2}\,,$$
$$q_{(-1/2)} = \frac{1}{2}\left(i\omega_1/P^*\right)\left(i\omega_0/P^* + k_f^2\right)^{-1/2}\,, \qquad (C.4)$$

and appropriate expansions for the coefficients b_i are written as

$$b_i \sim b_i^{(-2)}\epsilon^{-2} + b_i^{(-3/2)}\epsilon^{-3/2} + \cdots\,, \quad i = 1,\, 2,\, 8\,, \qquad (C.5)$$

$$b_i \sim b_i^{(-3/2)}\epsilon^{-3/2} + b_i^{(-1)}\epsilon^{-1} + \cdots\,, \quad i = 3,\, 4,\, 5,\, 6,\, 7\,. \qquad (C.6)$$

Substituting these expansions into Eqs. (40) - (48) and equating coefficients of like powers of ϵ, we obtain

$$ik_{1,f}\, b_3^{(-3/2)} + ik_{2,f}\, b_5^{(-3/2)} + q_{(-1)}\, b_7^{(-3/2)} = 0\,, \qquad (C.7)$$

$$ik_{1,f}\, b_4^{(-3/2)} + ik_{2,f}\, b_6^{(-3/2)} + r_{(-1/2)}\, b_8^{(-2)} = 0\,, \qquad (C.8)$$

$$b_2^{(-2)} = -k_f/\rho^*\,, \qquad (C.9)$$

$$ik_{2,f}\left[b_3^{(-3/2)} - b_4^{(-3/2)}\right] - ik_{1,f}\left[b_5^{(-3/2)} - b_6^{(-3/2)}\right] = 0\,, \qquad (C.10)$$

$$b_7^{(-3/2)} - \frac{k_f}{i\omega_0} b_1^{(-2)} = i\omega_0\,, \qquad (C.11)$$

$$-\rho^* b_8^{(-2)} + (\rho^* + A_p^*) b_2^{(-2)} = 0\,, \qquad (C.12)$$

$$\left(1 + \frac{2k_f^2 P^*}{i\omega_0}\right) b_1^{(-2)} + b_2^{(-2)} - 2P^* q_{(-1)} b_7^{(-3/2)} - 2b_8^{(-2)} = \gamma k_f^2\,, \qquad (C.13)$$

$$-\frac{ik_{1,f}}{k_f} b_2^{(-2)} - P^* q_{(-1)} b_3^{(-3/2)} + 2P^* k_f \frac{ik_{1,f}}{i\omega_0} b_1^{(-2)} - P^*\, ik_{1,f}\, b_7^{(-3/2)} = \frac{ik_{1,f}}{\rho^*}\,, \qquad (C.14)$$

$$-\frac{ik_{2,f}}{k_f} b_2^{(-2)} - P^* q_{(-1)} b_5^{(-3/2)} + 2P^* k_f \frac{ik_{2,f}}{i\omega_0} b_1^{(-2)} - P^*\, ik_{2,f}\, b_7^{(-3/2)} = \frac{ik_{2,f}}{\rho^*}\,, \qquad (C.15)$$

where Eq. (C.10) was obtained from the leading-order difference of Eq. (42) multiplied by $ik_{2,f}$ and Eq. (43) multiplied by $ik_{1,f}$, and Eq. (C.12) was obtained from the leading-order difference of Eqs. (44) and (45).

Equations (C.7) - (C.15) above constitute nine equations for the nine leading-order quantities $b_1^{(-2)}$, $b_2^{(-2)}$, $b_{3-7}^{(-3/2)}$, $b_8^{(-2)}$ and $i\omega_0$. Thus, from Eqs. (C.9), (C.12) and (C.13), we obtain

$$\left(1 + \frac{2k_f^2 P^*}{i\omega_0}\right) b_1^{(-2)} - \frac{k_f}{\rho^*} - 2P^* q_{(-1)} b_7^{(-3/2)} + \frac{2(\rho^* + A_p^*) k_f}{\rho^{*2}} = \gamma k_f^2\,, \qquad (C.16)$$

while the sum of Eq. (C.14) multiplied by $ik_{1,f}$ and Eq. (C.15) multiplied by $ik_{2,f}$, along with Eqs. (C.7) and (C.9), gives

$$\left[q_{(-1)}^2 + k_f^2\right] b_7^{(-3/2)} - \frac{2k_f^3}{i\omega_0} b_1^{(-2)} = 0\,. \qquad (C.17)$$

Hence, using the definition of $q_{(-1)}$, Eqs. (C.11) and (C.17) determine $b_1^{(-2)}$ and $b_7^{(-3/2)}$ as

$$b_1^{(-2)} = -\frac{i\omega_0}{k_f}(2P^* k_f^2 + i\omega_0)\,, \quad b_7^{(-3/2)} = -2P^* k_f^2\,. \qquad (C.18)$$

Substituting the results (C.17) and (C.18) into Eq. (C.16), we finally obtain the leading-order dispersion relation for $i\omega_0$ as

$$(i\omega_0)^2 + 4P^* k_f^2\, i\omega_0 - 4P^* k_f^3 \sqrt{i\omega_0 P^* + k_f^2 P^{*2}} = \frac{2k_f^2}{\rho^{*2}}(A_p^* - \hat{A}_p^*) - 4P^{*2} k_f^4\,, \qquad (C.19)$$

where $\hat{A}_p^*$ is given by the expression (55) for the leading-order inviscid cellular boundary $A_p^{*(f)}$ in the far outer wavenumber region, and the square root, which arises from the definition in (C.4) of $q_{(-1)}$, denotes the principal square root.

In the inviscid limit $P^* = 0$, we recover the leading-order results for the inviscid case. In particular, Eq. (C.19) reduces to $(i\omega_0)^2 = 2k_f^2(A_p^* - \hat{A}_p^*)/\rho^{*2}$, and hence $i\omega_0 > 0$ (unstable) for $A_p* > \hat{A}_p^*$ and is pure imaginary for $A_p^* < \hat{A}_p^*$. Stability in the latter region is thus determined by the coefficient $i\omega_1$ of the next term in the expansion (C.2), which, from either a continuation of the present calculation or from the direct expansion of the inviscid dispersion relation (49), is given by $i\omega_1 = (A_p^{*2} - \rho^{*2})/\rho^{*2}$. Consequently, the region $-\rho^* < A_p^* < \hat{A}_p^*$ is stable, while the region $A_p^* < -\rho^*$ is unstable, and identical results are obtained in the inner and outer wavenumber regimes. Hence, we recover both the steady (cellular) stability boundary $A_p^* = \hat{A}_p^*$ (on which $i\omega$ is identically zero) and the nonsteady (pulsating) stability boundary $A_p^* = -\rho^*$ (on which only the real part of $i\omega$ is zero) shown in Figures 2 and 3.

For $P^* > 0$, it is readily seen from Eq. (C.19) that the root $i\omega_0 = 0$ still corresponds to the inviscid cellular boundary $A_p^* = \hat{A}_p^*$, so that the cellular boundary is unchanged from its inviscid limit in the weakly viscous regime described by (C.1). On the other hand, it can be shown that the entire region $A_p^* < \hat{A}_p^*$ is now stable. This is most easily seen by considering the regime $0 < P^* \ll 1$ and seeking solutions $i\omega_0$ of Eq. (C.19) in the expanded form

$$i\omega_0 \sim i\alpha_0 + i\alpha_1 P^* + i\alpha_2 P^{*2} + \cdots\,. \qquad (C.20)$$

Then, at leading order with respect to the above expansion, we obtain the previous inviscid result (corresponding to $P^* = 0$),

$$(i\alpha_0)^2 = \frac{2k_f^2}{\rho^{*2}}(A_p^* - \hat{A}_p^*)\,, \qquad (C.21)$$

which implies instability only for $A_p^* > \hat{A}_p^*$, and neutral stability ($\text{Re}\{i\alpha_0\} = 0$) otherwise. At the next order, however, we obtain

$$i\alpha_0(i\alpha_1 + 2k_f^2) = 0\,, \qquad (C.22)$$

which implies stability ($i\alpha_1 = -2k_f^2 < 0$) in the region $A_p^* < \hat{A}_p^*$. Thus, in the A_p regime considered here, even very weak ($P^* \ll 1$) viscosity is sufficient to destroy the pulsating type of instability, at least in the far outer wavenumber region where viscous effects are first felt, whereas the cellular stability boundary is clearly unaffected even when $P^* \sim O(1)$. Indeed, the latter is modified only for O(1) values of the unscaled Prandtl number P, as described in the main body of the text.

Appendix D. The Pulsating Stability Boundary for Small Liquid Prandtl Numbers

For small liquid viscosities such that $P = \hat{P}\epsilon$, and the same scalings (52) and (62) as in the $P \sim$ O(1) case analyzed in the main body of the text, the effect of viscosity on the cellular boundary disappears at leading order [$P \to 0$ in Eqs. (100)], while the effect of viscosity on the pulsating boundary is only significant in the far outer wavenumber regime. In that case, the appropriate expansions analogous to Eqs. (101) – (106) are given by

$$i\omega \sim \epsilon^{-3/2}(i\omega_0 + i\omega_1\epsilon^{1/4} + i\omega_0\epsilon^{1/2} + \cdots)\,, \qquad (D.1)$$

$$r \sim r_{(-1/2)}\epsilon^{1/2} + O(\epsilon^{-1/4})\,, \quad r_{(-1/2)} = -i\omega_0\rho^*\,, \qquad (D.2)$$

$$q \sim q_{(-5/4)}\epsilon^{-5/4} + O(\epsilon^{-1})\,, \quad q_{(-5/4)} = \left(i\omega_0/\hat{P}\right)^{1/2}, \qquad (D.3)$$

$$b_i = b_i^{(-2)}\epsilon^{-2} + b_i^{(-7/4)}\epsilon^{-7/4} + b_i^{(-3/2)}\epsilon^{-3/2} + \cdots\,, \quad i = 1,\,2,\,8\,, \qquad (D.4)$$

$$b_i = b_i^{(-3/2)}\epsilon^{-3/2} + b_i^{(-5/4)}\epsilon^{-5/4} + \cdots\,, \quad i = 3,\,4,\,5,\,6\,, \qquad (D.5)$$

$$b_i = b_i^{(-5/4)}\epsilon^{-5/4} + b_i^{(-1)}\epsilon^{-1} + \cdots\,, \quad i = 7\,. \qquad (D.6)$$

Substituting these expansions into Eqs. (40) – (48) and equating terms corresponding to like powers of ϵ then gives, as previously, a sequence of equations for the recursive determination of the coefficients in the above expansions. Similar to the calculation for $P \sim$ O(1) in the outer wavenumber regime (Section 6), we obtain in this case that

$$(i\omega_0)^2 = \frac{2k_f^2}{\rho^{*2}}\left(A_p^* - \hat{A}_p^*\right)\,, \quad i\omega_1 = 0\,,$$
$$i\omega_2 = k_f\left[\left(\frac{A_p^*}{\rho^*}\right)^2 - 2\hat{P}k_f - 1\right]\,, \qquad (D.7)$$

where $\hat{A}_p^* = (\rho^*/2)(\rho^*\gamma k_f - 1)$ is the inviscid cellular boundary in the far outer wavenumber regime given by Eq. (55). The first of Eqs. (D.7) thus recovers the cellular stability boundary, but since $i\omega_0$ is purely imaginary for $A_p^* < \hat{A}_p^*$, stability in that region is determined by the real part of the next nontrivial coefficient in the expansion (D.1). Thus, setting $i\omega_2 = 0$ in the last of Eqs. (D.7), the pulsating stability boundary in the far outer wavenumber regime is given by

$$A_p^* = -\rho^*\sqrt{1 + 2\hat{P}k_f}\,, \qquad (D.8)$$

which, in the limit $k_f \to 0$, matches with the leading-order pulsating boundary $A_p^* = -\rho^*$ in the outer wavenumber region, which is unaffected by viscosity to this order of approximation. Thus, Eq. (D.8), which in terms of k is given by $A_p^* = -\rho^*\left(1 + 2\hat{P}\epsilon k\right)^{1/2}$, is valid for arbitrary wavenumbers. Writing $\hat{P}$ in terms of its unscaled counterpart P, this expression becomes identical to Eq. (129), which thus remains valid in the limit of small P.

Acknowledgement

This work was supported by the United States Department of Energy under contract DE-AC04-94AL85000 and by the NASA Microgravity Science Research Program under contract C-32031-E.

References

1. Zel'dovich, Ya. B., Barenblatt, G. I., Librovich, V. B., and Makhviladze, G. M., *The Mathematical Theory of Combustion and Explosions*, Consultants Bureau, New York, 1985.
2. Williams, F.A., *Combustion Theory*, Benjamin/Cummings, Menlo Park, 1985.
3. Vosen, S. R., "The Burning Rate of Hydroxylammonium Nitrate Based Liquid Propellants," *Twenty-Second Symposium (International) on Combustion*, The Combustion Institute, Pittsburgh, 1989, pp. 1817–1825.

4. Armstrong, R. C., and Margolis, S. B., "Hydrodynamic and Reactive/Diffusive Instabilities in a Dynamic Model of Liquid Propellant Combustion," *Twenty-Second Symposium (International) on Combustion*, The Combustion Institute, Pittsburgh, 1989, pp. 1807–1815.

5. Armstrong, R. C., and Margolis, S. B., "Hydrodynamic and Reactive/Diffusive Instabilities in a Dynamic Model of Liquid Propellant Combustion—II. Inviscid Fluid Motions," *Combust. Flame*, Vol. 77, pp. 123–138, (1989).

6. Landau, L. D., "On the Theory of Slow Combustion," *Acta Physicochimica URSS*, Vol. 19, pp. 77–85 (1944) & *Zh. Eksp. i Teor. Fiz.*, Vol. 14, p. 240 (1944).

7. Levich, V. G., "On the Stability of the Flame Front When a Liquid is Burning Slowly," *Dokl. Akad. Nauk SSSR*, Vol. 109, pp. 975–978 (1956).

8. Margolis, S. B., Sivashinsky, G. I., and Bechtold, J. K., "Secondary Infinite-Period Bifurcation of Spinning Combustion Waves Near a Hydrodynamic Cellular Stability Boundary," *Physica D*, Vol. 43, pp. 181–198 (1990).

9. Bechtold, J. K., and Margolis, S. B., "Nonlinear Hydrodynamic Stability and Spinning Deflagration of Liquid Propellants," *SIAM J. Appl. Math.*, Vol. 51, pp. 1356–1379 (1991).

10. Timnat, Y. M., *Advanced Chemical Rocket Propulsion*, Academic Press, London, 1987.

11. Margolis, S. B., and Sivashinsky, G. I., "On Spinning Propagation of Cellular Flames," *Combust. Sci. Tech.*, Vol. 69, pp. 99–131 (1990).

12. Margolis, S. B., and Sivashinsky, G. I., "Flame Propagation in Vertical Channels: Bifurcation to Bimodal Cellular Flames," *SIAM J. Appl. Math.*, Vol. 44, pp. 344–368 (1984).

13. Erneux, T., and Reiss, E. L., "Splitting of Steady Multiple Eigenvalues may Lead to Periodic Cascading Bifurcation," *SIAM J. Appl. Math.*, Vol. 43, pp. 613–624 (1983).

14. Buckmaster, J. D., "Polyhedral Flames—an Exercise in Bimodal Bifurcation Analysis," *SIAM J. Appl. Math.*, Vol. 44, pp. 40–55 (1984).

15. Margolis, S. B., "Hydrodynamic Instability in an Extended Landau/Levich Model of Liquid-Propellant Combustion at Normal and Reduced Gravity, *Combust. Flame*," to appear (1998).

16. Margolis, S. B., "On Pulsating and Cellular Forms of Hydrodynamic Instability in Liquid-Propellant Combustion," to appear (1998).